

Exploring decadal beach profile dynamics in response to nourishment strategies under accelerated sea level rise

Kettler, Tosca; de Schipper, Matthieu; Lujendijk, Arjen

DOI

[10.1016/j.ocecoaman.2024.107477](https://doi.org/10.1016/j.ocecoaman.2024.107477)

Publication date

2024

Document Version

Final published version

Published in

Ocean and Coastal Management

Citation (APA)

Kettler, T., de Schipper, M., & Lujendijk, A. (2024). Exploring decadal beach profile dynamics in response to nourishment strategies under accelerated sea level rise. *Ocean and Coastal Management*, 260, Article 107477. <https://doi.org/10.1016/j.ocecoaman.2024.107477>

Important note

To cite this publication, please use the final published version (if applicable). Please check the document version above.

Copyright

Other than for strictly personal use, it is not permitted to download, forward or distribute the text or part of it, without the consent of the author(s) and/or copyright holder(s), unless the work is under an open content license such as Creative Commons.

Takedown policy

Please contact us and provide details if you believe this document breaches copyrights. We will remove access to the work immediately and investigate your claim.



Exploring decadal beach profile dynamics in response to nourishment strategies under accelerated sea level rise

Tosca Kettler^{a,*}, Matthieu de Schipper^a, Arjen Luijendijk^{a,b}

^a TU Delft, Netherlands

^b Deltares, Netherlands

ARTICLE INFO

Keywords:

Nourishment strategies
Sand dispersion
Numerical modelling
Diffusion model
Cross-shore profile

ABSTRACT

Accelerated sea level rise prompts the upscaling of nourishment strategies, either through larger individual nourishment volumes or increased frequency of implementation. In such strategies, the nourished sand may lack time to effectively redistribute in the designated timeframe, leading to significant deformation of the profile over multiple nourishment cycles. This study quantifies subsequent effects, focusing on profile steepening, nourishment lifetimes, and the feasibility of operational objectives. We simulated two common nourishment strategies at a Dutch case study location using the cross-shore morphological model Crocodile over a 50-year timespan under sea level rise rates of 2–32 mm/year. The choice of strategy led to a variation of up to 75% in the total amount of sand used. Our results show increasing profile deformation with nourishment volume applied and duration of the nourishment strategy, with sand accumulating in the nourished section and little dissipation to the lower shoreface. The consequent profile steepening leads to reduced nourishment lifetimes by up to 30%. Additionally, under high sea level rise rates, more erosive coasts experience a reduction in nourishment lifetimes to annual intervals, while less erosive areas require up to four times more sand than currently needed. These findings illustrate key dilemmas in the formulation of future nourishment strategies and highlight the importance of optimizing these strategies to account for sea level rise.

1. Introduction

The use of nourishments is widely adopted to protect low-lying coastal areas from coastal erosion and sea level rise. Planning of longer-term programs involving nourishment application encompasses various design considerations, including the volume of sand applied, the anticipated return period between nourishments, and the depth at which sand is added to the cross-shore profile. There are notable variations among countries in their coastal management practices concerning nourishment (Brand et al., 2022; Cooke et al., 2012; Defeo et al., 2009; Hanson et al., 2002). Some countries, such as Italy and France, apply nourishment mostly in a reactive strategy in response to local requirements. Typically, the need for nourishment revolves around mitigating erosion at the local scale to prevent coastline retreat, but it may also include creating space for recreation. Long-term planning, an overarching strategy, or regular monitoring of the coastline may not always be present in these cases. Other countries, such as Germany and the Netherlands, have established proactive long-term nourishment programs that involve operational objectives on factors such as the

volume of sand applied and coastal state indicators such as coastline position, beach width and sand volume in the profile (Brand et al., 2022; Hanson et al., 2002). For example, the Netherlands has established a strategic goal to “sustainably maintain flood protection levels and sustainably preserve functions of dune areas” (Lodder et al., 2020). This goal translates into a tactical approach to keep the sediment budget in the coastal system, extending from MSL-20 m (mean sea level, referred to as NAP (Normaal Amsterdams Peil) in Dutch studies) up to the inner dune row, in equilibrium with sea level rise. The operational objectives of this approach include guidelines on the position of the coast and the annual volume of sand to be nourished. The design and assessment of such a nourishment program necessitate regular monitoring of the bathymetry and a thorough understanding of the coastal system. Additionally, sand volumes applied are generally higher and therefore this approach is only feasible if sufficient sand and the financial resources required for the execution of the program are available (Hanson et al., 2002).

Presently, adapted long-term nourishment programs to mitigate higher rates of sea level rise are formulated and explored (Haasnoot

* Corresponding author.

E-mail address: t.t.kettler@TUDelft.nl (T. Kettler).

<https://doi.org/10.1016/j.ocecoaman.2024.107477>

Received 29 July 2024; Received in revised form 9 October 2024; Accepted 7 November 2024

Available online 20 November 2024

0964-5691/© 2024 The Authors. Published by Elsevier Ltd. This is an open access article under the CC BY license (<http://creativecommons.org/licenses/by/4.0/>).

et al., 2020; Rijkswaterstaat, 2020). These programs often involve significantly greater volumes of sand compared to present-day practices. For instance, Haasnoot et al. (2020) estimated that nourishment volumes up to 20 times larger than those currently employed may be necessary to address extreme sea level rise rates of 60 mm per year at the Dutch coast. Achieving this could involve upscaling either the individual nourishment volume, the frequency of return, or both. A widely accepted assumption in formulating such nourishment programs is that coastal profiles respond to nourishment by rapid adjustment to a (new) equilibrium shape incorporating the added sand volume (Bruun, 1954, 1962; McCarroll et al., 2021). From this viewpoint, the total amount of added sand is the primary concern for profile evolution, while specific design elements like cross-shore location, frequency of return, and individual nourishment volumes are considered less critical. The validity of this perspective hinges on the timescale of equilibration of the coastal profile in relation to the timescale and extent of profile deformation caused by nourishment. Such profile equilibration is realized under the force of waves, wind, and tidal currents, which do not uniformly affect the profile. The upper profile experiences higher energy levels compared to the lower part, resulting in varying rates of sand redistribution along the profile. Consequently, timescales for morphological adaptation in response to altered boundary conditions, such as nourishment implementation, range from hours around the waterline to millennia near the inner shelf (Stive and de Vriend, 1995).

Therefore, it can take several decades for nourished sand to reach slower responding (deeper) areas in the profile (Hands and Allison, 1991). In the same rationale, nourishments placed lower in the profile typically redistribute slower (Beck et al., 2012), requiring shoreface nourishment to be about 25% larger than beach nourishment volumes for similar impact (Stive et al., 1991). The rate and extent of nourishment redistribution increase with larger nourishment volumes (Gijssman et al., 2018), with finer nourishment grain sizes (Ludka et al., 2016), and may be influenced by the presence of geological or man-made structures (Faraci et al., 2013). Additional factors influencing sand redistribution are, amongst others, the profile shape (e.g. de Schipper et al., 2015; Liu et al., 2024), the wave climate and surfzone processes (Pang et al., 2020, 2021), the sand's mineralogical composition (Yao et al., 2024) and sorting processes (Duan et al., 2020).

In future nourishment scenarios involving higher nourishment volumes we hypothesize that the nourished sand may lack time to effectively redistribute in the designated timeframe. Over multiple nourishment cycles this can lead to significant deformation of the profile shape, such as widening of beaches and the steepening of the profile when nourished sand accumulates in the nourished profile section. Observations of such profile deformation effects have already been documented in the Netherlands, where several decades of nourishment have resulted in notable steepening of the profile (Rijkswaterstaat, 2020; van der Spek and Lodder, 2015).

Profile steepening has been suggested to shorten the lifespan of individual nourishments, as it can lead to increased wave energy levels higher in the profile, inducing accelerated sand dispersion from the active zone to the lower shoreface (Stive et al., 1991). However, no such acceleration was observed after implementing a mega nourishment, despite a 50% increase in submerged profile slope between MSL-3 and MSL-19 m (Taal et al., 2023). As repeated upper profile nourishment may at most cause a similar effect, it can be deduced that the dissipation of nourished sand to the lower shoreface will have a minor impact on nourishment feasibility. Therefore, there is little reason to require the lower shoreface to grow along with sea level rise for coastal safety purposes. For the Netherlands, which maintains a tactical approach of keeping the sediment budget in the coastal system with a lower limit at MSL-20 m, this lower limit could be adjusted to a shallower depth. This knowledge is relevant as a future concern in high-volume nourishment scenarios is the extensive usage of sand. The seabed of the North Sea might in high-volume nourishment scenarios lack sufficient mineable sand volumes for nourishment, and socio-economic developments may

compete for sand as a resource, such as for constructing infrastructure (Bendixen et al., 2019; Torres et al., 2017).

Yet, the extent to which future upscaled nourishment volumes disperse and their effects - such as profile steepening, reduced nourishment return periods, and challenges in achieving strategic goals - are minimally quantified in present-day literature. The recently developed cross-shore morphological model Crocodile (Kettler et al., 2024) is specifically designed to simulate decadal profile responses to repeated nourishment, providing an opportunity to quantify these effects. In this study, we use this model to explore the physical feasibility of nourishment strategies involving larger sand volumes. To this end, two nourishment strategies are formulated that represent two outer ends within the spectrum of nourishment programs currently deployed in different countries; a *hold-the-line strategy* as reactive approach with minimal sand usage, and a *sand balance strategy* as proactive option aiming to elevate the coastal system, stretching seaward as deep as MSL-20 m, along with sea level rise. With Crocodile, 50-year morphological simulations are performed wherein these strategies are applied at a Dutch case study location, under sea level rise rates ranging from 2 to 32 mm/yr.

Based on the simulations conducted, we explore the solution space to mitigate accelerated sea level rise within the boundaries of laterally uniform nourishment strategies. Our goal is to establish explicit time-dependent relationships between nourishment strategy, sea level rise, and nourishment dispersion, with a specific focus on quantifying how much sand reaches the lower shoreface and addressing concerns about coastal steepening and reduced nourishment lifespan. We also simulate how different tactical approaches affect the volume of sand used. The insights gained aim to inform strategic decisions for nourishment programs, including the appropriate volume of sand to be applied as formulated within operational objectives.

This paper begins by detailing the relevant morphological and hydrodynamical characteristics of the central Holland coast, along with a description of the Dutch present-day operational nourishment programme (2.1). Hereafter, the numerical diffusion-based model Crocodile is briefly described (2.2), followed by an outline of the simulations performed which differ in rate of sea level rise and nourishment strategy (2.3). For all simulations, we explore the cross-shore profile dynamics and nourishment efficiency (3) and discuss insights and implications that can be drawn from the results (4). Finally, the paper concludes (5) by summarizing the main findings and evaluating the effectiveness of the simulated nourishment scenarios under different rates of sea level rise.

2. Methods

2.1. Case study

Our case study location is located along the Dutch sandy coast, a densely populated delta region where protection against relative sea level rise is crucial to prevent socio-economic disasters. A central region, the Holland Coast, was selected because of its well-documented and intensive local nourishment policy, and the extensive monitoring program providing yearly altimetric and bathymetric profile measurements (Wijnberg and Terwindt, 1995). Within this region, we adopt an unnourished coastal profile at the beach town called Monster (Fig. 1) as initial profile for our simulations.

2.1.1. Site description

The Holland coast consists of sandy beaches and dunes with an average tidal range of about 1.6 m (Wijnberg and Terwindt, 1995). The nearshore zone is characterized by a gradual sloping beach profile, occasionally interspersed with periodic nearshore bars. The shoreface slopes vary alongshore between 1:160 and 1:400, and slopes in the breaker zone vary from about 1:50 to 1:150 (Wijnberg and Terwindt, 1995).

Due to the rising sea level, soil subsidence and a declining sedi-

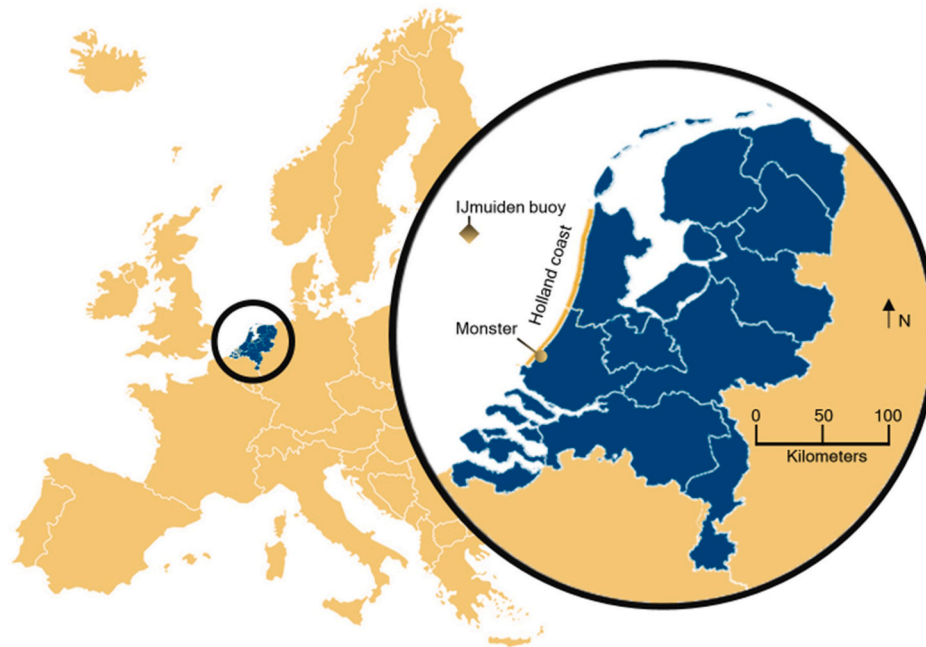


Fig. 1. – Location of case study site along the sandy Dutch coast and the IJmuiden wave station used for the long-term wave data.

mentary input from marine and riverine sources this coastal area has an erosive character. Therefore, the Dutch government executes a proactive nourishment program, wherein the main strategic goal is to maintain sustainable flood protection (Lodder et al., 2020). This program locally adheres to a hold-the-line approach, where the primary objective is to maintain the coastline seaward from a reference line (Van Koningsveld and Mulder, 2004). This reference line, known as the basal coastline ‘BCL’, has been determined based on the coastline position between 1980 and 1990. The momentary coastline ‘MCL’ serves as a volume-based proxy for the current shoreline position and is to be preserved seaward from the BCL. The position of the MCL is determined by calculating a weighted average of the cross-sectional profile volume A (in m^3/m alongshore) between the horizontal dune foot position (X_{df}) and the low water line plus the same elevation (h) below the low water line (Fig. 3D). It is expressed in meters relative to the BCL:

$$MCL = \frac{A}{2h} + X_{df} \quad (1)$$

The adoption of this volume-based approach aims to avoid that local small-scale variations in profile height, such as intertidal sand bars, result in large fluctuations in MCL (Van Koningsveld and Mulder, 2004). The MCL position is evaluated each year, and nourishments are carried out when it is landward of the BCL or anticipated to cross the BCL in the following year (Brand et al., 2022).

Since 2000, a second criterium has been used to maintain the sediment budget in the coastal system in equilibrium with sea level rise (SLR). Based on Mulder (2000) estimates of regarding the annual sediment demand in the coastal system, this is realized by the operational objective to annually nourish 12 million m^3 sand. For future sea level rise scenarios, the annual sediment demand V_{sd} is calculated as follows (Q. Lodder and Slinger, 2022):

$$V_{sd} = A_{cf} * SLRr + V_{sub} + V_e \quad (2)$$

In this equation, A_{cf} represents the planform surface area of the coastal foundation (in m^2) which is the coastal area that is wished to grow along with sea level rise, defined as the area between MSL -20 m up to the inner dune row. Thereby, A_{cf} is regarded as the active profile on multiple-decadal timescales. $SLRr$ denotes the local relative sea level rise

rate, expressed in m/yr . V_{sub} includes the local sediment demand (in m^3/yr) caused by sand extraction and anthropogenically induced subsidence due to the extraction of gas, oil, and salt. Both are not accounted for in the definition of relative sea level rise. V_e includes the net export of sand (in m^3/yr) from the coastal foundation area over its boundaries. This includes the sand export to the tidal inlets along the Dutch coast (Wadden sea, Western Scheldt) and the potential net export over the Dutch borders.

It is not established in the operational objectives how and where the added volume V_{sd} should be nourished. Typically, sand is added to depths shallower than MSL - 8 m, either directly onto the beach for beach nourishment or between MSL-4 and MSL-8 m for shoreface nourishment. The quantity and type of nourishment supplied vary per location and depend on various factors such as the current condition of the beach and dune system, anticipated future changes, and the preferences of local stakeholders. As not every location is suitable or desirable for nourishment, some nourishment locations receive additional sand to ensure that the volumetric target, annual nourishing V_{sd} , is reached.

2.2. The model: crocodile

With the numerical diffusion-based model Crocodile (Kettler et al., 2024), we conduct 50-year morphological simulations of a coastal transect with bed level $Z(x, t)$, with x referring to the horizontal coordinate and t referring to time. This model has specifically been developed to simulate effects of nourishment strategies on coastal profile evolution over a multiple-decadal timeframe (e.g. Fig. 2). Crocodile has been built upon the philosophy that the introduction of a nourishment essentially constitutes a perturbation to a coast, having a particular dynamic state (similar to models developed by e.g. Chen and Dodd, 2021, 2019; Coelho et al., 2017; Marinho et al., 2017; Stive et al., 1991). Over sufficiently long temporal and spatial scales, this perturbation is diffused in cross-shore and longshore directions. Thereby, a continuous and gradual adaptation of the coastal profile takes place towards a ‘dynamic equilibrium’ profile $Z_{eq}(x, t)$. This profile represents the theoretical shape and position the coastal profile would attain if all physical forces (waves, winds and tidal currents) and boundary conditions (sea level elevation and sand budget) in the coastal system

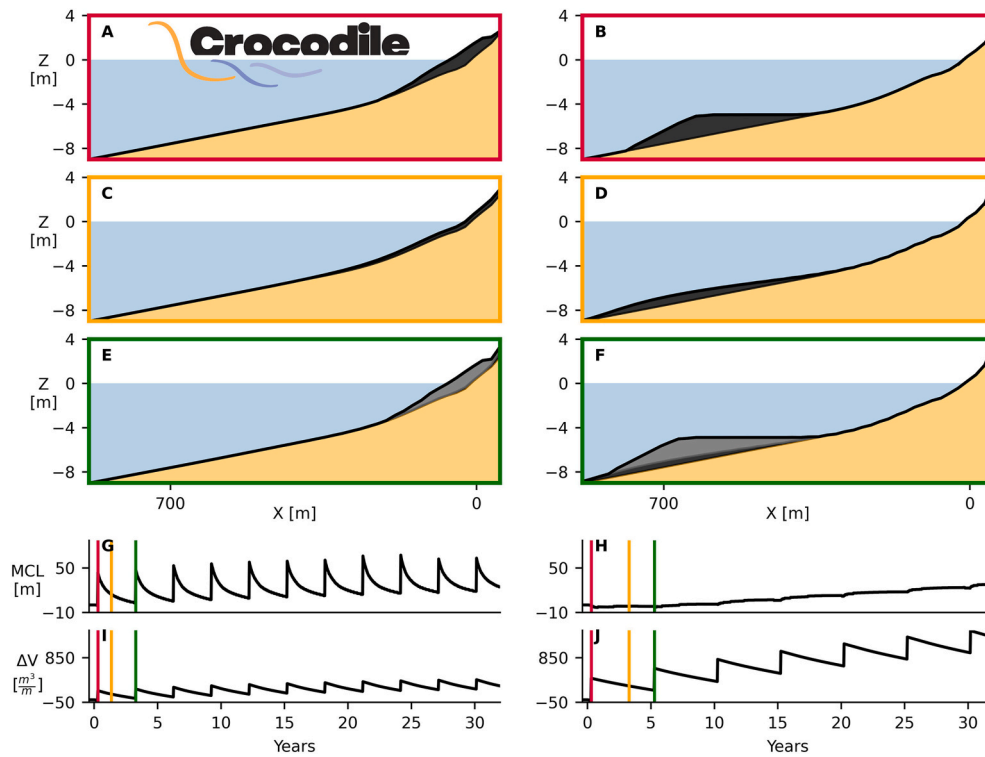


Fig. 2. – Simulated profile behaviour for 2 nourishment strategies by Crocodile. Left: 200 m³/m beach nourishment is applied every 3 years. Right: 450 m³/m shoreface nourishments every 5 years. The upper three rows display the evolution of bed level $Z(x,t)$ at different times in a nourishment cycle (times are indicated by the coloured lines in the timeseries in the lower panels). Bottom two rows show the temporal evolution of shoreline position MCL-BCL and profile cross-sectional volume ΔV . The peaks in ΔV and the corresponding responses in MCL-BCL arise from the implementations of individual nourishments.

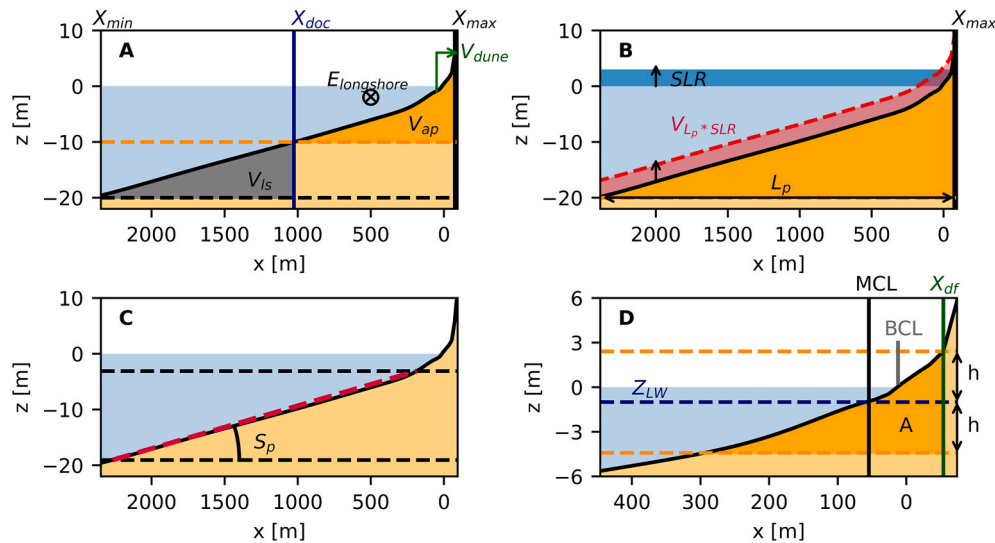


Fig. 3. Overview of evaluated parameters. A) Two volumetric profile sections V_{ap} (in orange) and V_{ls} (in grey), which are horizontally constrained by the horizontal positions X_{min} , X_{doc} and X_{max} in the initial profile. Sand fluxes $E_{longshore}$ and V_{dune} are indicated with arrows. B) The required volume to elevate the profile with sea level rise $V_{L_p * SLR}$ for profile length L_p . C) Submerged profile slope S_p . D) Momentary coastline MCL and basis coastline BCL. The profile section between the orange dashed lines is utilized to compute MCL and is also referred to as the MCL zone.

remained constant with time. Changes in these boundary conditions (e.g., sea level rise, alongshore transport gradients, or the implementation of nourishments) lead to horizontal and vertical translation of $Z_{eq}(x,t)$ as given by a sediment volume balance. The translation of the profile due to sea level rise is modelled based on the principles established by Bruun (1954, 1962), whereby $Z_{eq}(x,t)$ is raised by the change in sea level and shifted onshore to balance total sediment volume.

Every timestep t , Crocodile computes the ‘instantaneous’ bed level $Z(x,t)$ being the time-dependent profile approaching the dynamic equilibrium profile $Z_{eq}(x,t)$. The rate and extent of sand dispersion in $Z(x,t)$ depend on the vertical difference between $Z(x,t)$ and $Z_{eq}(x,t)$ as well as z' , being the profile depth relative to the mean sea level MSL:

$$\frac{d(Z - Z_{eq})}{dt} = \frac{d}{dx} \left\{ D(z') \frac{d(Z - Z_{eq})}{dx} \right\} + \varepsilon_D(z) + E(z') + F(Z - Z_{ini}) + W(Z - Z_{eq}) + \text{Source}(z', t) \quad (3)$$

The first and second RHS components of Eqs. (3) and (4) describe cross-shore diffusion, with $\varepsilon_D(z)$ being a correction term for volume conservation. These elements have varying time-dependent effects on cross-shore development (Kettler et al. (2024), Fig. 1). By inclusion of a diffusion coefficient, $D(z')$, the dependency of time-dependent profile dynamics on water depth z' is incorporated. $D(z')$ represents the average sediment redistribution capacity along the profile and thereby regulates the morphological timescale of response. It determines the rate and extent of cross-shore sand diffusion and thereby has a key role in both the time-dependent nourishment dispersion, as well as the depth-dependent coastal adaptation to sea level rise. The shape of $D(z')$ is prescribed as a function of boundary conditions and the local hydrodynamic climate, facilitating easy implementation of locations with different hydrodynamic characteristics in Crocodile. The third and fourth components on the RHS of eqs. (3) and (4) represent longshore sand losses, the fifth component describes sand exchange with the dune, and nourishments are incorporated as a source term.

The model is behaviour-oriented, meaning that the model components are formulated to optimally simulate the evolution of the cross-shore profile without aiming to resolve the underlying physics other than mass-conservation. As we consider a nourishment as a profile perturbation and assume a 'dynamic equilibrium' background profile, any autonomous (nourishment-independent) profile development affecting the profile shape is not resolved. This means that cycles of storm and recovery, cyclic bar behaviour and the passage of alongshore shoreline undulations are not included. The model was validated using three Dutch case study locations in Kettler et al. (2024), reproducing the decadal evolution of bulk parameters such as beach width, shoreline position, and coastal volume for nourishment strategies with varying nourishment volumes and cross-shore placement. On average, volumetric trends were overestimated by $1.5 \text{ m}^3/\text{m}/\text{yr}$ (7%), while modelled coastline trends were $0.2 \text{ m}/\text{yr}$ (15%) lower than observed. A more detailed description of the model and the validation study is available in Kettler et al. (2024).

2.2.1. Profile schematization

All simulations start from the same initial profile, which is derived from a set of yearly alti- and bathymetric surveys at Monster over an unnourished period (1966–1979), obtained from the JARKUS dataset (Wijnberg and Terwindt, 1995). The initial profile (both $Z(x, t = 0)$ and $Z_{eq}(x, t = 0)$) is a smoothed multi-year average from these surveys, such that sub-decadal autonomous coastal behaviour (e.g., storm cycles, cyclic bar behaviour) is excluded. This approach allows us to avoid selecting a theoretical definition of Z_{eq} , which would otherwise necessitate making assumptions about hydrodynamic conditions (Dean, 1991), sediment characteristics (Yao et al., 2024), and other environmental factors that could introduce uncertainties into determining the equilibrium profile.

The slope of the resulting initial profile in the 'active' zone between MSL - 10 m and the dune foot (MSL + 3 m) is 1:115. The dune front is represented by a linear slope extending from the dune foot Z_{df} to the upper model boundary Z_{max} , with the slope equal to the dune slope observed between MSL +4 and MSL +6 m, which was 1:3.875 at Monster.

2.2.2. Parametrization

The temporal resolution in the numerical scheme dt is 1/10 year, the spatial resolution in the cross-shore dx is 20 m. The mean water level is set $MWL(t = 0) = \text{MSL} + 0 \text{ m}$. All hydrodynamic and morphodynamic parameter values are obtained from literature concerning the central Dutch coast, equal to Kettler et al. (2024). Because of its importance for the outcomes, we highlight the key parameter related to cross-shore

diffusion and erosion, diffusion coefficient $D(z')$. To define $D(z')$, both a maximum value D_{max} is required, as well as hydrodynamic statistics to define its depth-dependency. The maximum of $D(z')$, D_{max} , is adopted from De Vriend et al. (1993), who estimated that $D_{max} = 60 \text{ m}^2/\text{day}$ for the central Dutch coast. $D(z')$ has this maximum value in the surf zone, and its magnitude over the remainder of the profile is a fraction of D_{max} based on offshore wave height and water level statistics obtained from the IJmuiden wave station located 35 km offshore (Fig. 1). Total background erosion rate $E_{longshore}$ is fixed at $40 \text{ m}^3/\text{m}/\text{yr}$ in our simulations. During the period from 1750 to 1980, the coastline retreat near Monster was about 300 m (Dillingh and Stolk, 1989). Assuming an active profile height of 30 m (from -20 MSL to +10 MSL), it can be inferred that a representative long-term total background erosion is approximately $300 * 30 / 230 \approx 40 \text{ m}^3/\text{m}/\text{yr}$.

2.2.3. Nourishment design parameters

The design height, landward slope, and seaward slope of the implemented nourishments are based on prevalent Dutch values as described by Brand et al. (2022). Hereby we distinguish between beach nourishments and shoreface nourishments. Both are implemented with triangular cross shore shapes, comprising a near horizontal platform and a linear slope towards the nourishment toe. For beach nourishments the platform connects with the original profile at elevation $H_n = \text{MSL} + 2 \text{ m}$. The landward slope is $S_{lw} = 1 : 200$ and the seaward slope S_{sw} is taken equal to the intertidal slope of $Z_{eq}(x, t = 0)$ between high water level $z'_{HW} = \text{MSL} + 1 \text{ m}$ and low water level $z'_{LW} = \text{MSL} - 1 \text{ m}$:

$$S_{sw} = \frac{Z_{HW} - Z_{LW}}{X_{eq}[Z_{HW}] - X_{eq}[Z_{LW}]} \quad (4)$$

Whereby $X_{eq}[z']$ refers to the horizontal position of the equilibrium profile intersecting with depth z' . For the profile at Monster $S_{sw} = 1:40$. Shoreface nourishments are implemented with $H_n = \text{MSL} - 5 \text{ m}$, $S_{lw} = 1 : 10000$ and $S_{sw} = 1 : 50$.

2.2.4. Evaluated coastal indicators

Crocodile computes the evolution of instantaneous bed level elevation $Z(x, t)$, which is translated into a set of coastal indicators. To analyse the dispersion of the nourished sand in our simulation, we examine changes in the volume of sand stored in two vertically constrained profile sections (Fig. 3A). The lowest section represents the volume of the lower shoreface and its change ΔV_{ls} is given by integrating the change in $Z(x, t)$ over this section:

$$\Delta V_{ls} = \int_{X_{min}}^{X_{doc}} (Z(x, t) - Z(x, t = t_0)) dx \quad (5)$$

The upper section represents the active profile and its change ΔV_{ap} is given by:

$$\Delta V_{ap} = \int_{X_{doc}}^{X_{max}} (Z(x, t) - Z(x, t = t_0)) dx \quad (6)$$

The change in total profile volume ΔV_p is then equal to the sum of ΔV_{ls} and ΔV_{ap} :

$$\Delta V_p = \Delta V_{ls} + \Delta V_{ap} \quad (7)$$

In these definitions, X_{min} is the seaward model boundary, positioned at $Z(X_{min}, t = 0) = \text{NAP} - 20 \text{ m}$ in this work. The horizontal position X_{doc} represents the depth of closure in the initial profile, serving as a boundary between the active profile and lower shoreface. We approximate its depth at $Z(X_{doc}, t = 0) = \text{NAP} - 10 \text{ m}$ in this application (Hinton and Nicholls, 1998). X_{max} is the landward horizontal position where $\frac{dz}{dt} = 0$ throughout the simulations, approximately positioned at $Z(X_{df},$

$t = 0) = NAP + 6 \text{ m}$. Two sinks of sand outside the modelled profile exist, which are direct outputs from the model. These are ΔV_{dune} , which is the cumulative volume of sand transported towards the dunes, and the volume that has eroded longshore $E_{longshore}$. We compare ΔV_{ls} , ΔV_{ap} , ΔV_{dune} and $E_{longshore}$ to the cumulative total nourished volume ΣV_N :

$$\Sigma V_N = \sum_{t=0}^t V_N dt \quad (8)$$

Wherein V_N is the individual nourishment volume. Additionally, we compute the required profile volume change ΔV_{L_p*SLR} to elevate the profile with sea level rise (SLR) (Fig. 3B):

$$\Delta V_{L_p*SLR} = L_p * SLR \quad (9)$$

With L_p being the profile length between X_{min} and X_{max} . Comparing V_{L_p*SLR} to the sum of ΔV_{ls} and ΔV_{ap} shows how the sand budget in the profile evolves with respect to sea level rise. If these two are equal, the sand budget is sufficient for this profile to grow along. Additionally, we analyse the position of the MCL with respect to BCL , which is determined as $BCL = MCL(t = 0)$ in the current analysis. Herein X_{df} is positioned at $Z(x, t = 0) = 3\text{m}$. Moreover, the submerged profile slope S_p between $z' = MSL(t) - 19$ and $z' = MSL(t) - 3$ is evaluated to quantify profile steepening (Fig. 3C):

$$S_p = 16 / (X[z' = MSL(t) - 19, t] - X[z' = MSL(t) - 3, t]) \quad (10)$$

The slope of the initial profile $Z(x, t = 0)$ is given by:

$$S_{ini} = S_p(t = 0) \quad (11)$$

2.3. Scenarios

2.3.1. Sea level rise scenarios

We consider a set of stationary sea level rise rates (SLRr): 2, 4, 8, 16 and 32 mm/yr, which is hereafter referred to as $SLRr2$, $SLRr4$, $SLRr8$, $SLRr16$ and $SLRr32$. These rates remain constant throughout the simulation for simplicity. Thereby, we avoid specifying when in time this occurs, which is inherently uncertain. The sea level rise rates are based

on expected sea level rise rates in the Netherlands over the next century, estimated by KNMI (2023) (see appendix A1). The KNMI scenarios provide the context for the sea level rise rates adopted in this research. $SLRr2$ reflects conditions over the past decades, $SLRr4$ serves as an estimate for the next decade, $SLRr8$ is anticipated several decades from now, and $SLRr16$ may be approached near the end of this century under high emissions. $SLRr32$ is included to explore extremities, without pre-tending high likelihood of occurrence.

2.3.2. Nourishment scenarios

We established conceptual nourishment scenarios, categorized in two subsets based on different operational objectives. The first subset follows a 'proactive sand balance strategy' with predefined nourishment volumes inspired by the present-day Dutch nourishment program (Fig. 4 – left column). The second subset of conceptual nourishment scenarios adopts a 'reactive hold-the-line strategy' (Fig. 4 – right column). Both subsets are simulated twice under all different sea level rise rates (2.3.1.), whereby nourishments are either repeatedly placed directly on the beach or as shoreface nourishment.

2.3.2.1. Proactive sand balance strategy. The first subset of conceptual nourishment scenarios follows a 'proactive sand balance strategy', where nourishments are planned based on expected sand losses and SLR. The modelled scenarios use predefined nourishment volumes in line with the present-day Dutch nourishment program (depicted in Fig. 4A and B). Presently, adapted proactive sand-balance strategies are formulated to define the coastal zone management of the Netherlands under climate change (Haasnoot et al., 2020, RWS kustgenese2.0). These strategies estimate future annual nourishment volumes required to elevate the coastal foundation zone, stretching seaward as deep as $MSL - 20 \text{ m}$, along with sea level rise. By simulating such scenarios, we aim to study potential constraints when upscaling the current Dutch nourishment program with larger volumes of sand.

We hypothesized earlier that sand may accumulate in the nourished area if the nourished sand does not effectively redistribute within the designated timeframe, leading to beach widening and profile steepening. Therefore, we evaluate to what extent the upscaled nourishment

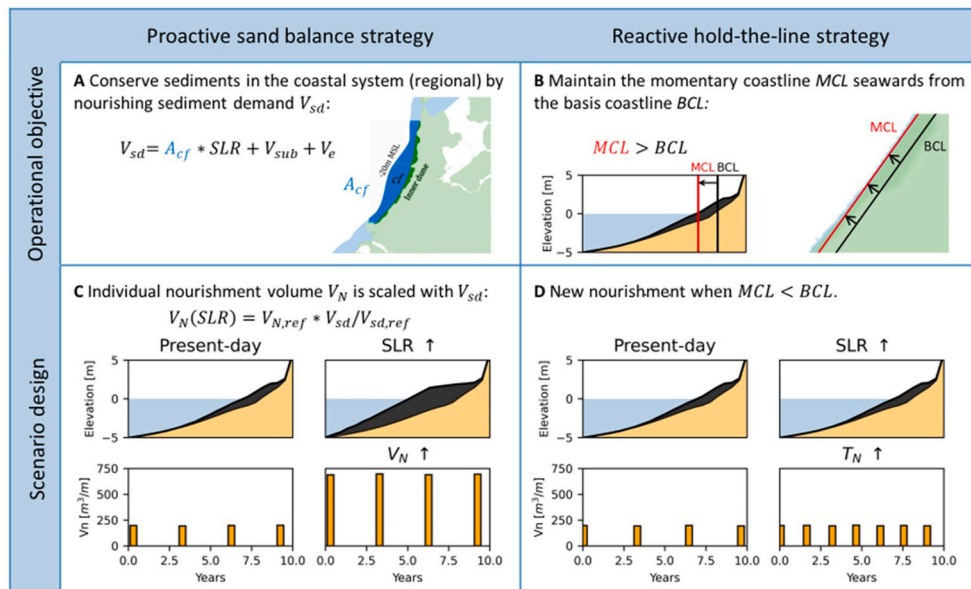


Fig. 4. – Schematic illustration of the operational objectives and scenario design for the nourishment scenarios established in this research. (A) The operational objective for the proactive sand balance strategy is to conserve sediments in the regional coastal system by nourishing sediment demand V_{sd} . This includes the volume of sand required to elevate the coastal foundation area A_{cf} , stretching seaward as deep as $MSL - 20 \text{ m}$, along with sea level rise, and compensate for subsidence V_e and sand loss due to erosion V_e . (B) The operational objective for the reactive hold-the-line strategy is to maintain the momentary coastline MCL seawards from the basis coastline BCL . (C) The scenario design adopted in the proactive sand balance strategy is to upscale individual nourishment volume V_N proportionally in relation to V_{sd} under accelerated sea level rise. (D) The scenario design adopted in the reactive hold-the-line strategy is to place a new nourishment when the MCL crosses landwards from the BCL .

volumes spread over the whole design area (i.e. the coastal foundation zone over its full depth). Moreover, if the nourishment accumulates high in the profile, we assess how much the beach widens over time ($MCL - BCL$) and how much the profile steepens (ΔS_p). Furthermore, by comparing $V_{L_p^*SLR}$ to the sum of ΔV_{ls} and ΔV_{ap} we assess whether the sediment budget in the profile balances with sea level rise, and thereby whether the design objective is fulfilled.

We follow a top-down methodology, where the local nourishment volume in the considered transect is determined based on the sediment demand in the coastal foundation area (A_{cf}). The strategic goal is to raise A_{cf} in response to sea level rise. The required volume of sand for this purpose, sediment demand V_{sd} , is defined using Eq. (2) for the different rates of sea level rise. We base the equation components on (Rijkswaterstaat, 2020), with the adoption of $A_{cf} = 702 \text{ km}^2$ (Rijkswaterstaat, 2020 Tles 6-2) for the central Dutch coast, and $V_e + V_{sub} = 2.568 \text{ mln m}^3/\text{yr}$. Consequently, V_{sd} amounts to $3.972 \text{ mln m}^3/\text{yr}$ for $SLRr2$, approximately doubling for $SLRr8$, and escalating to over six times as large for $SLRr32$ (Table 1).

To design nourishment scenarios at our case study site, we must make assumptions about the distribution of V_{sd} along the coast. In the Netherlands, nourishment is typically concentrated in specific locations known as erosional hotspots, characterized by higher erosion rates compared to the surrounding areas. Conversely, other locations are not suitable or desirable to receive nourishment. Additional nourishments are occasionally placed at the erosional hotspots to ensure that the volumetric target of annual nourishing V_{sd} , is reached. We presume our case study transect to be one such location, and we assume the continuity of this policy.

As a result, our scenarios incorporate nourishment volumes that surpass the average sediment demand per meter longshore in the region. This demand can be computed by dividing V_{sd} by the total length of the central Dutch coast L_c (V_{sd}/L_c wherein $L_c = 107 \text{ km}$). For $SLRr2$, V_{sd}/L_c is $37 \text{ m}^3/\text{m}/\text{yr}$, equivalent to beach nourishment volumes of $121 \text{ m}^3/\text{m}$ every 3 yr or shoreface nourishments of $185 \text{ m}^3/\text{m}$ every 5 yr. These values are notably smaller than the average nourishment applications at nourished sites in the Netherlands over the past few decades. As reported by Brand et al. (2022), beach nourishments in the Netherlands have an average individual volume of $200 \text{ m}^3/\text{m}/\text{yr}$ with a 3-yr return period and shoreface nourishments have average volumes of $450 \text{ m}^3/\text{m}/\text{yr}$ with a 5-yr return period. This disparity between the average

Table 1

– Nourishment options for different SLRr scenarios. From top to bottom: SLRr - rate of sea level rise; $V_e + V_{sub}$ - volumes of exported sand V_e and anthropogenically induced subsidence V_{sub} ; A_{cf}^*SLR - volume of sand needed to elevate the coastal foundation zone A_{cf} with sea level rise; V_{sd} - total sediment demand; $V_{sd}/V_{sd,ref}$ - nourishment upscaling ratio; $V_N \text{ Beach}$ - beach nourishment volume (for a constant return period of 3 yr); $V_N \text{ Shoreface}$ - shoreface nourishment volume (for a constant return period of 5 yr); $T_N \text{ Beach}$ - beach nourishment return period (for a constant nourishment volume of $200 \text{ m}^3/\text{m}$); $T_N \text{ Shoreface}$ - shoreface nourishment return period (for a constant nourishment volume of $450 \text{ m}^3/\text{m}$).

SLRr (mm/yr)	2	4	8	16	32
$V_e + V_{sub}$ (mln m ³ /yr)	2,6	2,6	2,6	2,6	2,6
A_{cf}^*SLRr (mln m ³ /yr)	1,4	2,8	5,6	11,2	22,5
V_{sd} (mln m ³ /yr)	4,0	5,4	8,1	13,8	25,0
$V_{sd}/V_{sd,ref}$	1,0	1,4	2,1	3,5	6,3
$V_N \text{ Beach}$ (m ³ /m)	200	271	412	695	1260
$T_N = 3 \text{ yr}$					
$V_N \text{ Shoreface}$ (m ³ /m)	450	609	927	1563	2836
$T_N = 5 \text{ yr}$					
$T_N \text{ Beach}$ (yr)	3,0	2,2	1,5	0,9	0,5
$V_N = 200 \text{ m}^3/\text{m}$					
$T_N \text{ Shoreface}$ (yr)	5,0	3,7	2,4	1,4	0,8
$V_N = 450 \text{ m}^3/\text{m}$					

sediment demand and actual nourishment volumes arises from the uneven distribution of nourishments along the Dutch coast.

We formulate two conceptual present-day strategies for our case study site grounded in the findings of Brand et al. (2022). One involves beach nourishment of $200 \text{ m}^3/\text{m}/\text{yr}$ every 3 yr, and the other involves shoreface nourishment of $450 \text{ m}^3/\text{m}/\text{yr}$ every 5 yr. Recalculated to yearly sand usage, the applied beach nourishment amounts to $66 \text{ m}^3/\text{m}/\text{yr}$, and the applied shoreface nourishment is higher with $90 \text{ m}^3/\text{m}/\text{yr}$. These values can be adjusted for different sea level rise while maintaining a constant frequency of nourishment. Then the individual nourishment volume V_N is proportionally upscaled in relation to V_{sd} :

$$V_N(SLR) = V_{N,ref} * V_{sd}/V_{sd,ref} \quad (12)$$

Here, $V_{N,ref}$ and $V_{sd,ref}$ respectively represent the nourishment volumes and sediment demand under $SLRr2$. With eqs. (8) and (12), individual nourishment volumes are, similar to V_{sd} , doubled for $SLRr8$, and sixfold for $SLRr32$ (Table 1). While such large cross-sectional nourishment volumes have been implemented before (Brand et al., 2022; Valloni and Médit, 2007), there are no known locations where such large volumes have been consistently nourished at 3- or 5-year intervals.

It should be kept in mind that upscaling V_{sd} for sea level rise mitigation could also be realized by increasing the frequency of nourishment, instead of increasing individual nourishment volumes. Nevertheless, for the computed sediment demand opting for an increase in frequency is anticipated to be an unfavourable strategy for ecological and socio-economic reasons (M. A. De Schipper et al., 2021). The sediment demand under high sea level rise namely demands a significantly shortened return period T_N . For example, under $SLRr8$, T_N decreases to approximately 1.5 years for beach nourishment and 2.4 years for shoreface nourishment (Tables 1 and 2 lowest rows). Moreover, adjusting frequency shows similar outcomes as increasing individual nourishment volume for the evaluated coastal indicators within the presented approach. Therefore, only the volume upscaled scenarios are presented hereafter.

2.3.2.2. Reactive hold-the-line strategy. The alternative nourishment strategy explored is the commonly employed hold-the-line approach (Fig. 4 – right column). In contrast to what we refer to as a ‘proactive strategy’, the frequency of nourishment is not predetermined in this case. The individual nourishment volumes for this approach remain at $200 \text{ m}^3/\text{m}$ for beach nourishments and $450 \text{ m}^3/\text{m}$ for shoreface nourishments through all simulations. In the hold-the-line simulations, we stipulate that, within the nourished transect, the MCL should remain seawards from the BCL . To this end, a new nourishment is placed directly before the coastline crosses landwards from its initial position. Although this approach could as well be classified as a proactive strategy, a key difference is that regularly bed level observations determine the implementation of nourishments. This approach aligns with common coastal management policies in, for example, Italy and France (Hanson et al., 2002).

The cumulative total nourished volume, ΣV_N , employed during these simulations is typically much lower than in the proactive scenarios, thereby representing a minimum amount of sand to keep the coastline ‘in place’ under a specific rate of sea level rise. By comparing ΣV_N between the two scenarios, we highlight the extent of this difference. Moreover, it is acknowledged that accelerated sea level rise increases the rate of coastline regression, which in this approach results in a reduction of the nourishment return period, T_N , as the volume of nourishment remains constant. This study contributes to understanding of this issue by quantifying reductions in T_N under accelerated sea level rise. Additionally, from these simulations we examine how the profile steepens and T_N evolves with scenario duration.

2.3.2.3. Background erosion by gradients in longshore transport. Within a

hold-the-line strategy, T_N varies significantly over different locations (e. g. Brand et al., 2022). In addition to sea level rise, T_N is influenced by factors such as the local hydrodynamic climate, sediment characteristics, tidal currents and the background erosion, i.e. the supply and loss of sediment through existing gradients in longshore transport (Nederbragt, 2006). Additionally, within the same location, nourishment return periods fluctuate over time due to temporal variability in these factors. This variability may stem from natural sources like variations in storminess and sediment supply from rivers. Furthermore, human interventions can induce more permanent changes in sediment supply (e. g. Almar et al., 2015).

We investigate one of these dependencies; the variation in supply and loss of sediment through gradients in longshore transport $E_{longshore}$, defined as the amount of sand loss in cubic meter per longshore meter, with units of $m^3/m/yr$. To investigate the relation between T_N and $E_{longshore}$, we perform additional 50-year simulations with longshore erosion rates $E_{longshore}$ ranging from -10 to $-70 m^3/m/yr$ under the same set of $SLRr$ scenarios.

3. Results

3.1. Proactive sand balance strategy

3.1.1. Simulated behaviour for beach nourishment scenarios

The simulations with a duration of fifty years show sand accumulation in the nourished section, resulting in a growing deformation of the cross-shore profile that increases with both scenario duration and the rate of sea level rise (Fig. 5A–E). In the proactive beach nourishment scenario under $SLRr2$, the beach is nourished with $200 m^3/m$ every 3 years, resulting in stepwise $200 m^3/m$ increases in ΔV_{ap} (Fig. 5F). The major portion (90%) of this added sand disperses in the subsequent

years, spreading either in longshore direction ($\Delta E_{longshore}$ in Fig. 5F) or beyond the landward boundary of the profile (ΔV_{dune} in Fig. 5F). Throughout the simulation no sand reaches the lower shoreface in this scenario, as $\Delta V_{ls} = 0$. The average annual volumetric increase in ΔV_{ap} over the successive nourishment cycles amounts to $6 m^3/m/yr$, closely aligning with ΔV_{ip*SLR} , which is $8 m^3/m/yr$. The MCL thereby migrates hardly seawards (appr. 20 m, Fig. 5K).

For the simulations wherein $SLRr$ exceeds $4 mm/yr$, the increase in ΔV_p (Eq. (7)) is larger than V_{ip*SLR} , exceeding the necessary volume to elevate the profile with sea level rise (Fig. 5G–J). In addition, the profile gradually steepens (Fig. 5P–T) and the MCL migrates seaward with each nourishment over the successive nourishment cycles (Fig. 5K–O). These trends are more pronounced at higher $SLRr$, indicating that the lateral sand dispersion does not proportionally increase with the larger nourishment volumes. While under $SLRr2$ only 10% of ΣV_N remains in ΔV_p , this increases to 20% ($SLRr4$), 40% ($SLRr8$), 60% ($SLRr16$) and 80% ($SLRr32$). As the simulations mainly differ in the volume of nourishment applied, we find a non-linear, decreasing relationship between nourishment volume ΣV_N and sand dispersion rates ΔV_p .

The phenomenon of profile steepening and seaward MCL migration due to the accumulation of nourishments high in the profile is subsequently referred to as ‘upper profile obesity’ (best visible in Fig. 5D–E). The extent of profile steepening under present-day sea level rise rates ($SLRr2/SLRr4$) is moderate, but under higher $SLRr$ the profile steepening increases when larger volumes of nourishment are applied in a shorter timeframe, whereby the profile slope increases with scenario duration. For example, in 50 years under $SLRr8$ the initial submerged profile slope S_p of 1:133 increases to 1:108 (+23%, Fig. 5R).

The upper profile obesity leads to increased dispersion rates, resulting in reduced annual growth of ΔV_{ap} as the scenario duration increases. We observe minimal influx of sand into the lower shoreface.

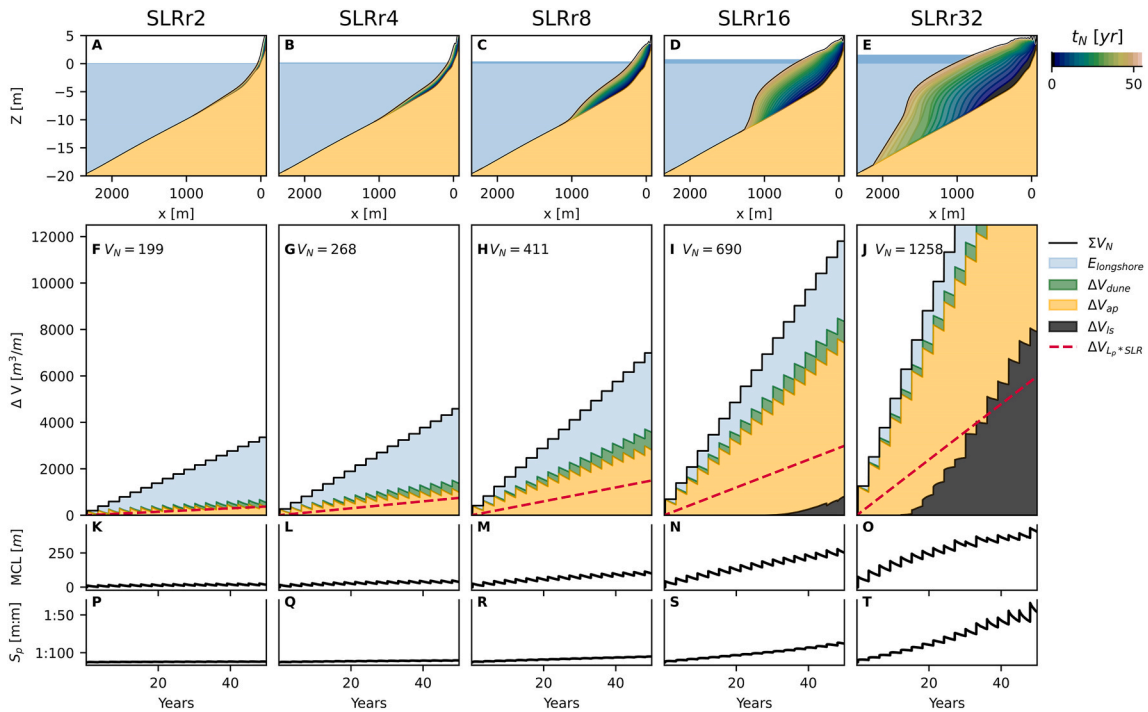


Fig. 5. Proactive beach nourishment scenarios. Each column represents a scenario with the rate of sea level rise indicated by “ $SLRr$ ” + the head number (in mm/yr). Panels A–E show the profile shape and sea level after 50 years whereby the sand-coloured profile represents the initial profile and the blue/green colours the sand from successive individual nourishments placed at year t_N indicated by the colour bar on the right. Panels F–J represent the cumulative nourished volume ΣV_N and shows the part of it that is eroded ($E_{longshore}$) and the part that is stored in different profile sections. The latter is subdivided in the dune volume (ΔV_{dune}), the active profile volume (ΔV_{ap}) and the lower shoreface volume (ΔV_{ls}). The red dashed line represents the volume required to elevate the total profile with SLR (V_{ip*SLR}). If this line equals $\Delta V_{ap} + \Delta V_{ls}$ ($= \Delta V_p$, see Eq.6), there is sufficient sand in the profile (to grow along with SLR). Panel K–O represent the MCL compared to the BCL (positioned at $x = 0$ m). Panel P–T show the submerged profile slope S_p , measured between $MSL-3$ and $MSL-19$ m.

Although ΔV_p exceeds V_{lp*SLR} , this sand is stored in ΔV_{ap} and ΔV_{ls} does not grow along with SLR , a phenomenon we term ‘lower shoreface starvation’ hereafter. If the predetermined nourishment volumes are adhered to when upper profile obesity develops, nourishments are positioned further seaward due to constraints on available space within the initial active profile. After several decades of beach nourishment under $SLRr16$ and $SLRr32$, nourishments are ultimately placed beyond the seaward boundary of the initial active profile. The latter can be observed in Fig. 5d-e, where the expansion of ΔV_{ls} aligns with ΣV_N .

3.1.2. Simulated behaviour for shoreface nourishment scenarios

The simulations with shoreface nourishments show sand accumulation in the nourished section, resulting in a growing deformation of the cross-shore profile that escalates with both scenario duration and the rate of sea level rise (Fig. 6A–E). In the proactive scenario involving repeated shoreface nourishment under $SLRr2$, the shoreface is nourished with $450 \text{ m}^3/\text{m}$ every 5 years, resulting in stepwise $450 \text{ m}^3/\text{m}$ increases in ΔV_{ap} (Fig. 6F). The sand reaches the beach as it redistributes along the profile, with a portion dispersing longshore and over the landward boundary. The portion of ΣV_N that remains in the profile after 45 years is 32%. This translates to an average annual increase in ΔV_p by $28 \text{ m}^3/\text{m}/\text{yr}$, approximately 4.5 times more than in the beach nourishment scenario, and much more than ΔV_{lp*SLR} (Fig. 6F). The remaining 68% of ΣV_N is transported either longshore or beyond landward boundary of the profile. As the nourishments are placed outside the MCL zone (Fig. 3C), their individual effect on the MCL is lagging the nourishment implementation. In this scenario, the MCL is relatively stable, with 20 m seaward migration (Fig. 6K).

For the scenarios with $SLRr$ exceeding $4 \text{ mm}/\text{yr}$, we see how the nourishment strategies become affected by the sand redistribution capacity along the profile. While under $SLRr2$ only 32% of ΣV_N remains in ΔV_p , this increases to 44% ($SLRr4$), 59% ($SLRr8$), 74% ($SLRr16$) and 86% ($SLRr32$) (Fig. 6F–J). In the scenarios with $SLRr$ exceeding $8 \text{ mm}/\text{yr}$, this accumulation becomes so substantial that the available space for placing nourishments becomes limited and nourishments are being placed outside the initial active profile. This can be observed in Fig. 6H–J by the stepwise growing ΔV_{ls} . Nevertheless, the larger nourishments still induce larger onshore sand fluxes. The MCL migration 50 years is 46 m under $SLRr2$ and increases to 66 m ($SLRr4$), 98 m ($SLRr8$), 128 m ($SLRr16$) and 210 m ($SLRr32$) (Fig. 6K–O).

3.2. Reactive hold-the-line strategy

3.2.1. Simulated behaviour for beach nourishment scenarios

The beach nourishment scenarios following a reactive hold-the-line strategy prove highly cost-effective concerning the volume of sand used to counteract MCL retreat. Total nourished volume ΣV_N in these scenarios is considerably smaller than in the proactive scenarios. Under $SLRr2$, it is roughly one third smaller, and under $SLRr8$, ΣV_N is half as large, and under $SLRr32$ scenario, it diminishes to a quarter (Fig. 11A). We observe that this is an insufficient amount of sand for ΔV_p to grow along with ΔV_{lp*SLR} for all scenarios. While ΔV_{ap} fluctuates around its initial value for $SLRr2$ and $SLRr4$ and grows slightly with scenario duration under higher $SLRr$, there is no growth of the lower part of the profile ($\Delta V_{ls} = 0$) across all scenarios (Fig. 7F–J).

The impact on the profile shape induced by the nourishments is consequently less pronounced than in the proactive beach nourishment scenarios (compare Fig. 7A–E to Fig. 7A–E). Under $SLRr2$ and $SLRr4$, the profile returns to its initial shape after each nourishment cycle. As a result, the return period T_N between the nourishments is stable over these scenarios (Fig. 7U and V). In $SLRr2$ scenario, T_N is approximately 4 years. In contrast, under $SLRr8$ and higher $SLRr$, sand accumulates in the nourished section and the profile steepens (Fig. 7R–T). In scenarios $SLRr8$, $SLRr16$ and $SLRr32$, S_p respectively increases from the initial value 1:129 to 1:126 (3%), 1:122 (6%), and 1:112 (15%) over the 50 years of simulation. This leads to an increase in longshore and cross-shore sand dispersion with scenario duration inducing a gradual reduction of T_N . In the case of $SLRr32$, this results in a decrease in T_N from about 3 to under 2 years, equivalent to a 25%–50% reduction compared to $SLRr2$ (Fig. 7Y). In section 3.2.3 we delve further into this profile steepening and subsequent reduction in T_N .

3.2.2. Simulated behaviour for shoreface nourishment scenarios

In the shoreface nourishment scenarios following a reactive hold-the-line strategy, the nourishments are positioned seawards from the MCL zone. Compared to the proactive approach, ΣV_N is reduced by approximately equivalent proportions as for the reactive versus proactive beach nourishment scenarios (Fig. 11B). Consequently, the growth of ΔV_p is slower than ΔV_{lp*SLR} , as the sand does not reach the lowest parts of the profile sufficiently to elevate with SLR (Fig. 8I–J). As shoreface nourishments enhance the sand budget in the MCL zone with a time delay,

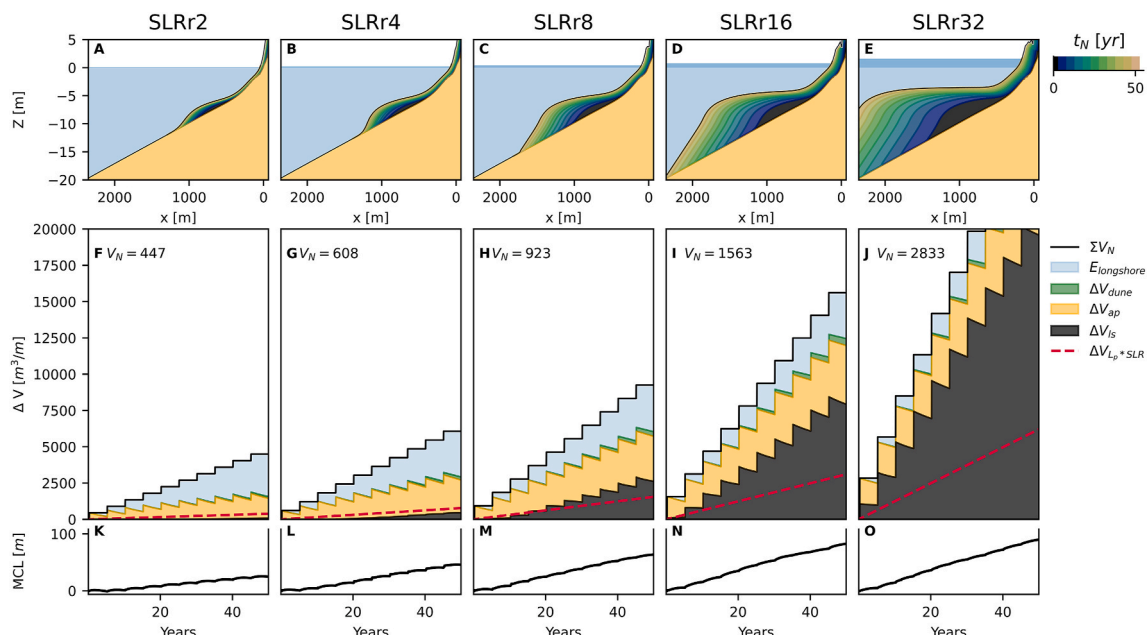


Fig. 6. Proactive shoreface nourishment scenarios. For descriptions of panel contents, the reader is referred to Fig. 5.

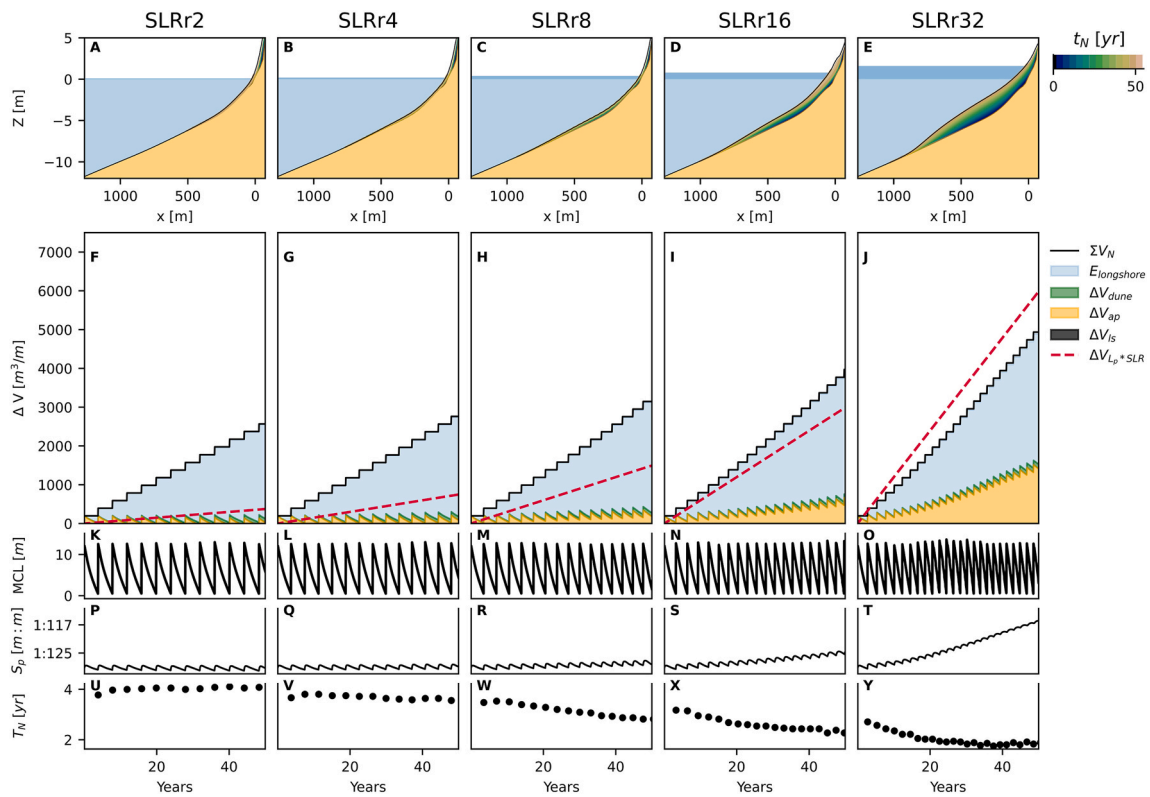


Fig. 7. Reactive hold-the-line beach nourishment scenarios. Each column represents a scenario with the rate of sea level rise indicated by “SLRr”+the head number (in mm/yr). Panels A–E show the profile shape and sea level at the end of each simulation whereby the sand-coloured profile represents the initial profile and the blue/green colours the successive individual nourishments. Panels F–J represent the cumulative nourished volume ΣV_n and shows the part of it that is eroded ($E_{\text{longshore}}$) and the part that is stored in different profile sections. The latter is subdivided in the dune volume (ΔV_{dune}), the active profile volume (ΔV_{ap}) and the lower shoreface volume (ΔV_{ls}). The red dashed line represents the volume required to elevate the total profile with SLR ($V_{\text{lp}^{\text{SLR}}}$). If this line equals $\Delta V_{\text{ap}} + \Delta V_{\text{ls}}$ ($= \Delta V_{\text{p}}$, see Eq.6), there is sufficient sand in the profile to grow along with SLR. Panel K–O represent the MCL compared to the BCL. Panel P–T show the submerged profile slope S_p , measured between MSL-3 and MSL-19 m. Panel U–Y show the nourishment return period T_N .

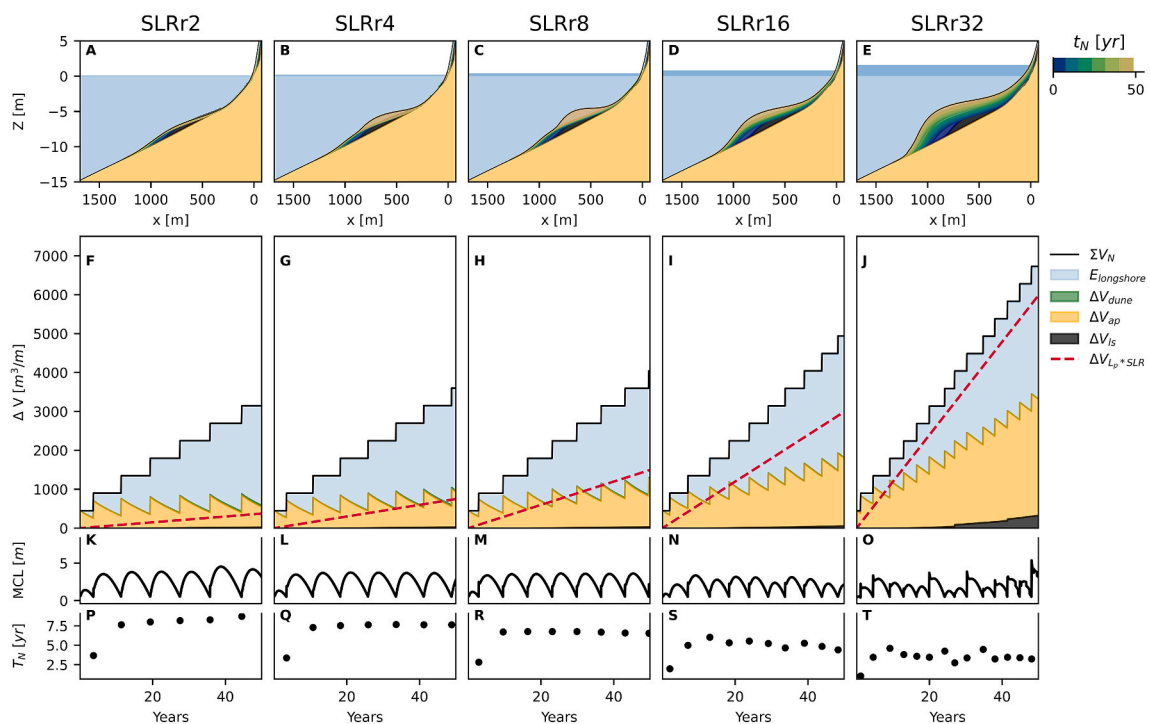


Fig. 8. – Reactive hold-the-line shoreface nourishment scenarios. For descriptions of panel A–O contents the reader is referred to Fig. 7. Panel P–T show the nourishment return period T_N .

the first nourishment is relatively less effective counteracting MCL retreat (Fig. 8F–J). The resulting landward sand supply is then insufficient to counteract SLRr and longshore erosion, which drive the MCL inland. Therefore, shortly after the first nourishment, a second one is implemented to preserve the coastline.

Both for the first nourishment as for the remainder of the simulation T_N reduces significantly with increasing SLRr (Fig. 8P–T). While the average T_N under SLRr2 is 7.4 years, the average T_N in SLRr32 is 4 years (55%) shorter. T_N roughly stabilizes after the second nourishment in simulations with the lowest SLRr, once dispersion rates reach their maximum. In SLRr16 and SLRr32, sand accumulates in the nourished area over the course of the simulation. Similar to the proactive shoreface nourishment scenarios, the accommodation space of nourishment then declines in these scenarios with largest SLR rates. Therefore, the nourishments are placed further seawards, leading to a reduction of effectiveness as cross- and longshore sand redistribution is slower. Consequently, T_N slightly declines over the successive nourishment cycles (Fig. 8S and T).

3.2.3. Profile steepening and nourishment lifetime reduction

Earlier, we briefly addressed the degree of profile steepening in the proactive (Fig. 5P–T) and reactive (Fig. 8P–T) beach nourishment scenarios. In both cases, the steepening leads to increased rates of longshore and cross-shore nourishment dispersion. In the reactive case this is most evident as it results in a subsequent reduction in nourishment lifetime T_N . Therefore, we use reactive simulations to further explore this relation. To this end, we extend the reactive beach nourishment strategy simulations to 200 years or until MSL surpasses $NAP + 2m$. Profile steepening is expressed as the change in submerged profile slope ($S_p - S_{ini}$). The relative reduction in T_N compared to lifetime of the first nourishment in the simulation, $T_{N,first\ nourishment}$, is given by:

$$\Delta T_N[\%] = 100 * T_N(t) / T_{N,first\ nourishment} \quad (13)$$

We analyse the relationships between the value of ($S_p - S_{ini}$) at the last timestep before nourishment placement and $\Delta T_N[\%]$ of that nourishment. Under various SLRr, these relationships are similar, whereby $\Delta T_N[\%]$ declines as ($S_p - S_{ini}$) increases (Fig. 9A). We note an asymptotic trend around a 30% reduction in T_N under the higher SLRr. This point is reached after 100 years under SLRr 8 or after 50 years for SLRr16, when the profile has steepened by about 8% (from 1:129 to 1:120). However, under SLRr2 and SLRr4, this asymptote remains elusive within the 200-year timeframe.

To extrapolate this finding into a broader context, we fit an exponential curve between S_{ini} , the profile slope increase ($S_p - S_{ini}$), and $\Delta T_N[\%]$:

$$\Delta T_N[\%] = a * \left(\exp \left(- \left(\frac{b}{S_{ini}} \right) * (S_p - S_{ini}) \right) - 1 \right) \quad (14)$$

Utilizing a non-linear least squares algorithm to minimize the variance between Eq. (11) and (14) and the simulation data, we determine the parameters as $a = 32$ and $b = 34$, yielding an R^2 value of 0.64.

To explore the sensitivity of this relationship to different sites with S_{ini} , we analyse an alternate set of beach nourishment simulations, this time over a less steep profile characterized by an initial slope $S_{ini} = 1 : 201$. This profile is derived from a set of yearly alti- and bathymetric surveys at the Dutch coastal town Katwijk over an unnourished period (1966–1998), sourced from the JARKUS dataset (Wijnberg and Terwindt, 1995). The simulations with this profile reveal similar T_N reductions over time, albeit with a more moderate degree of profile steepening (Fig. 9B). Nevertheless, in percentages compared to the initial profile slope, the profile steepening is similar. Repeating the fitting procedure for the Katwijk data with Eq. (11) and (14) yields

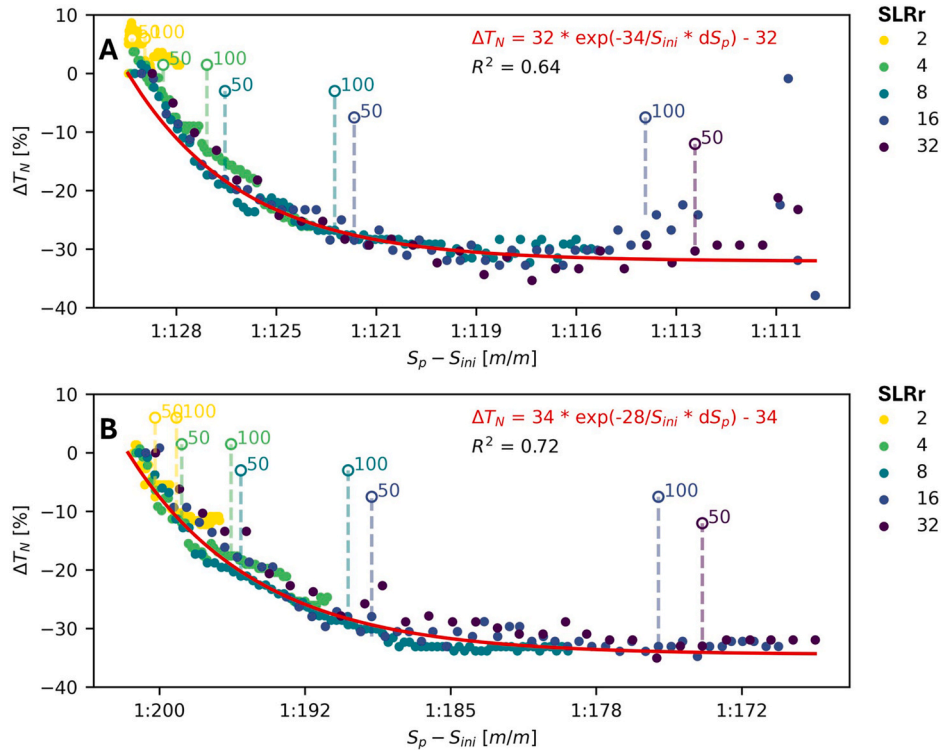


Fig. 9. – Change in beach nourishment return period ΔT_N reduction as a function of increase in submerged profile slope $S_p - S_{ini}$ under various SLR rates distinguished by different colours. The scattered data points are derived from the reactive hold-the-line beach nourishment simulations at (A) Monster and (B) Katwijk, where each dot indicates the T_N and pre-placement ($S_p - S_{ini}$) of an individual beach nourishment. Nourishments placed approximately 50 and 100 years into the simulation timeframe are indicated by the dashed lines. The nonlinear least-squares fit, minimizing the difference between the data and Eqs. (11) and (14), is depicted in red.

parameters $a = 34$ and $b = 28$ with an R^2 value of 0.72. Given that a and b are of comparable magnitude for both the initial profiles at Monster and Katwijk, we infer that Eq. (11) and (14), with approximate values $a \approx 33$ and $b \approx 31$, can effectively estimate the anticipated reduction in T_N attributed to profile steepening for the range of slopes evaluated.

These findings confirm that steepening of the coastal profile leads to faster beach nourishment redistribution and a reduction in T_N over time, but suggest that it becomes significant only after several decades of frequent nourishment and under sea level rise rates exceeding 8 mm/yr. In these scenarios, our simulations show a reduction in return periods over time by up to 30% due to coastal steepening, in addition to the reduction caused by increased sea level rise rates. Under low SLRr, T_N is sufficiently long to allow the profile to roughly return to its original shape. Thereof, we conclude that at present, profile steepening is unlikely to significantly decrease T_N .

3.2.4. Impact of the existing gradients in longshore transport

Nourishment efforts are generally focused on locations where a negative longshore gradient in sand transport is present. Model results presented in the previous sections included this alongshore effect with a magnitude of $E_{longshore} = -40 \text{ m}^3/\text{m}/\text{yr}$. In this section we research the influence of $E_{longshore}$ on nourishment dissipation. We adopt the reactive hold-the-line strategy for this analysis, as the nourishment dissipation in this strategy is quantifiable through a subsequent reduction in nourishment lifetime T_N . To evaluate the influence of $E_{longshore}$ on T_N , we present the results of an alternate set of reactive hold-the-line simulations with longshore erosion rates $E_{longshore}$ varying from -10 to $-70 \text{ m}^3/\text{m}/\text{yr}$. As T_N varies over a single simulation, we evaluate the average T_N of all nourishments implemented within the 50-year timeframe.

We observe that T_N decreases for both increasing SLRr and increasing $E_{longshore}$, as illustrated in Fig. 10. The influence of $E_{longshore}$ is largest for low SLRr; for beach nourishments under SLRr2, the average T_N decreases significantly from 4 to 2.5 year (-38%) if $E_{longshore}$ is increased from $-40 \text{ m}^3/\text{m}/\text{yr}$ to $-70 \text{ m}^3/\text{m}/\text{yr}$ (Fig. 10A, left column). Such dependence of T_N on $E_{longshore}$ is less prominent for larger SLRr. Under SLRr32, T_N is reduced from 2 to 1.5 year (-25%) when comparing $E_{longshore} = -70 \text{ m}^3/\text{m}/\text{yr}$ to $-40 \text{ m}^3/\text{m}/\text{yr}$ (Fig. 10A, right column). Shoreface nourishments exhibit similar relationships between $E_{longshore}$ and T_N . Comparing shoreface nourishments under $E_{longshore} = -70 \text{ m}^3/\text{m}/\text{yr}$ to $-40 \text{ m}^3/\text{m}/\text{yr}$, T_N is reduced from 7.5 to 4.3 year (-43%) under SLRr2 (Fig. 10B, left column), and from 3.4 to 2.5 year (-26%) under

SLRr32 (Fig. 10B, right column). These results highlight the dependency of T_N on the $E_{longshore}$, recognizing it as another major contributor to long-term coastline retreat, alongside sea level rise. Moreover, the results underline that T_N may vary over time due to temporal variability in $E_{longshore}$.

Additionally, we compare how the simulated T_N responds to accelerated SLR among locations with a given $E_{longshore}$ for SLRr2 versus SLRr32. In a highly erosive profile ($E_{longshore} = -70 \text{ m}^3/\text{m}/\text{year}$), the average return period decreases by 35% (from 2 to 1.3 years - Fig. 10A, lower row), while it decreases by 50% (from 4 to 2 years - Fig. 10A, centre row) under moderate $E_{longshore} = -40 \text{ m}^3/\text{m}/\text{year}$, and by 75% (from 11.3 to 2.8 years - Fig. 10A, upper row) under a very low $E_{longshore}$ of $-10 \text{ m}^3/\text{m}/\text{year}$. Thus, we observe that the difference in T_N between simulations with different $E_{longshore}$ diminishes with increasing SLRr. This shift occurs because, with increasing SLRr, the primary purpose to place nourishments shifts from counteracting structural erosion to mitigating sea level rise. This finding may be even more important for low-erosive beaches than for beaches under high erosion rates. Although return periods become shortest for highly erosive settings, the reduction in return period and subsequent increase in sand demand for nourishment is largest for less erosive coasts. These coasts are likely less well-monitored because there is little need at present, so for coastal management this may be a factor to consider in future.

4. Discussion

4.1. Considerations in selecting a nourishment strategy

In this section, we delve into the practical considerations of selecting an appropriate nourishment strategy in light of accelerated sea level rise. Our discussion is based on the findings from Chapter 3, and we aim to contextualize our points by directly linking them to the results and observations detailed in that chapter.

4.1.1. Comparison of sand volumes between strategies

To mitigate accelerated sea level rise, nourishment programs can increase the volume or frequency of nourishments (or a combination of both). Our study demonstrates that magnitude of the increase strongly depends on the operational objectives adopted in a nourishment program. In the pro-active sand balance nourishment approach presented, the total nourishment volume over a 50-year timespan doubles for SLRr8, and escalates over sixfold for SLRr32 (Fig. 11, blue bars marked "P"). Conversely, the reactive hold-the-line strategy involves considerably smaller sand volumes and raises, amounting to roughly two thirds

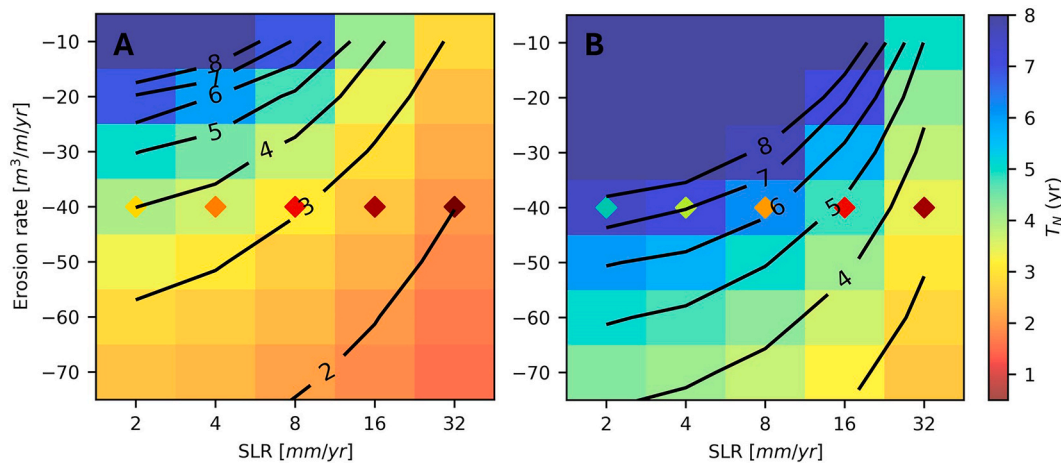


Fig. 10. Nourishment return period T_N under reactive hold-the-line (A) beach and (B) shoreface nourishment scenarios, as a function of sea level rise rate SLRr and longshore erosion rate $E_{longshore}$. T_N is defined as the time between nourishment implementation and the moment the MCL retreats landwards from the BCL. The coloured diamonds refer to computed T_N (Table 1) in proactive scenarios with increased frequency and present-day nourishment volumes.

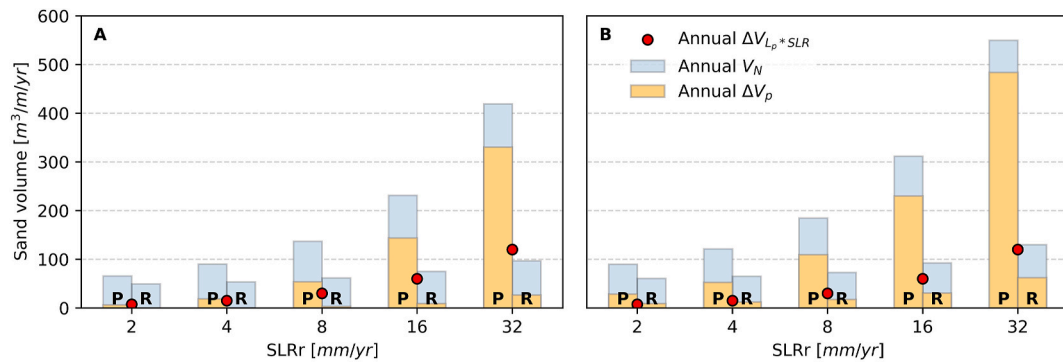


Fig. 11. – A volumetric comparison between the (A) beach and (B) shoreface nourishment for various SLRr scenarios as simulated. The P refers to the proactive sand balance scenarios, the R to the reactive hold-the-line scenarios. All volumes are averaged over 50 years of simulation. The graph includes annual nourished sand volume V_N and annual profile volume change ΔV_p . The red dots represent the volumes required to elevate the total profile with SLR (V_{lp*SLR}). If these equal ΔV_p , there is sufficient sand in the profile to grow along with SLR.

under *SLRr2* to a quarter under *SLRr32* compared to the proactive approach (Fig. 11, blue bars marked “R”). Thus, the difference between these approaches increases as sea level rise accelerates, underscoring the importance of sand availability and economic considerations in strategy selection.

4.1.2. Feasibility of operational objectives

We observe a limitation in achieving the operational objective of elevating large areas along with sea level rise by nourishment concentrated in specific locations, such as in the proactive strategy presented. Our results indicate that as nourishment volumes increase, sand dispersion rates do not keep pace, leading to accumulation in the nourished profile section. In case of beach nourishment, ‘upper profile obesity’ develops whereby the coast steepens and the lower shoreface remains largely unaffected. This is consistent with bathymetric studies in the Netherlands indicating limited dissipation of nourishments to the lower shoreface in recent decades resulting in a relatively steeper profile (Van der Spek and Lodder, 2015). We add to these findings that this remains the case under large nourishment volumes, confirming that the lower shoreface adaptation occurs over a considerably longer timescale compared to the application of nourishment. Consequently, it is not required that the lower shoreface grows along with sea level rise for coastal safety purposes.

In addition to the increased nourishment volumes, the insufficient nourishment redistribution under accelerated sea level rise is also partly attributable to a shift in the distribution of sand demand across the profile. With increasing sea level rise, the reason to place nourishments shifts from primarily counteracting structural erosion to primarily mitigating sea level rise. Both erosion and sea level rise increase the sediment demand of the profile, but the distribution of this demand across the profile differs. Structural erosion acts upon the profile according to the acting forces, with higher sand losses in the zone of wave breaking and along the coastline, and lesser impact on the lower shoreface. In contrast, sea level rise essentially reframes the profile, resulting in a profile-uniform ‘apparent’ loss of volume. In the context of structural erosion, it is logic to compensate for the total volumetric loss over the profile. However, under sea level rise, a computed sediment demand in a volume-based proactive strategy is contingent upon the profile length desired to grow along. Consequently, we anticipate that under severe rates of sea level rise, a revision of either the tactical goal or the nourishment design in such volume-based proactive strategies is inevitable.

Such a revision may include a thorough examination of the lowest elevation of the profile that is desired to grow with sea level rise. In line with this rationale, it has recently been proposed to restrict the seaward limit adopted within sand balance computations (A_{cf} in eq. (2)) to MSL-8 instead of MSL-20 m, significantly reducing the required nourishment

volumes as the area to be elevated is over five times smaller (Taal et al., 2023). Our study supports this proposal. If maintaining the current tactical goals is preferred, alternative nourishment approaches or sites for nourishment could be explored. Possible locations could involve neighbouring places that are not yet intensively nourished. Alternative methods might encompass mega nourishment projects (e.g. De Schipper et al., 2014), outer delta nourishment or pipeline nourishment. Taking a broader perspective, the proactive volume-based scenario simulations presented in this study highlight that an effective present-day nourishment policy may not necessarily be the optimal approach under accelerated sea level rise due to differences in sand demand, both in volume and distribution over the profile.

4.1.3. Sea level rise and nourishment lifetime reduction

We assessed how much the nourishment return frequency increases as a function of sea level rise and coastal erosion. Comparing hold-the-line simulations under *SLRr32* to *SLRr2* at our case study with moderate erosion rate (~ 40 m³/m/yr), the average nourishment return period reduces by about 50% for both beach and shoreface nourishment (from 4 to 2 years and from 7.4 to 3.4 years respectively) when individual nourishment volumes are unaltered. Coastal areas with higher erosion rates (~ 70 m³/m/yr) see return periods drop to annual intervals, while less erosive coasts face the largest reduction in return periods and require up to four times more sand than at present under *SLRr32*. To prevent the future shortening of nourishment lifespans in hold-the-line policies, increasing individual nourishment volumes may be advantageous.

4.1.4. Coastal steepening and nourishment lifetime reduction

Steepening of the profile occurs when beach nourishment accumulates in the upper profile section due to incomplete redistribution over the profile. The extent of profile steepening under present-day sea level rise rates (*SLRr2* or *SLRr4*) simulated in both strategies presented was moderate, aligning with observations in the Netherlands (Rijkswaterstaat, 2020; van der Spek and Lodder, 2015). Under higher *SLRr* the profile steepening increases when larger volumes of nourishment are applied in a shorter timeframe, whereby the profile slope increases with scenario duration. This steepening is consequently larger in the proactive than in the reactive strategy, due to the difference in sand volumes are applied. For example, in 50 years under *SLRr8* the initial submerged profile slope S_p of 1:133 increases to 1:108 (+23%) in the proactive scenario and to 1:115 (+16%) in the reactive case. Profile steepening has been raised as a concern, as has been suggested to shorten the lifespan of individual nourishments due increased wave energy levels higher in the profile leading to increased dune erosion (Stive et al., 1991). Our findings confirm this effect, but suggest that it becomes significant only after several decades of frequent nourishment

and under sea level rise rates exceeding 8 mm/yr. In these scenarios, our simulations show a reduction in return periods over time by up to 30% due to coastal steepening, in addition to the reduction caused by increased sea level rise rates.

4.2. Reflection on methods

In interpreting the outcomes of this study, it is crucial to recognize that our objective is to simulate expected coastal responses to decadal nourishment programmes, not to predict the actual coastal evolution on a day to day basis. As we consider the nourishments as profile perturbations and assume a ‘dynamic equilibrium’ background profile, any autonomous (nourishment-independent) profile development affecting the profile shape is not resolved. This means that cycles of storm and recovery, cyclic bar behaviour and the passage of alongshore shoreline undulations are not included in the model. Additionally, there are stochastic aspects of hydroclimatic influences (e.g., energetic vs moderate years) that the model, being stationary forced, cannot replicate. In many real-world scenarios, autonomous coastal developments often overshadow the effects of nourishment observed on short timescales. Consequently, the model cannot be utilized as a predictor or compute specific details of the cross-shore profile shape on short timescales. Instead, its primary capability lies in comparing the long-term profile responses between periods with different strategies of nourishment.

We acknowledge that the high rates of sea level rise and nourishment volumes used in this research exceed the conditions in the case studies used for model validation (Kettler et al., 2024). This discrepancy arises because no existing sites currently experience these conditions - which was also a key motivator for the present study. The gap between the validation cases and the modelled scenarios introduces significant uncertainty into the model’s outcomes, and we emphasize that the quantitative results should only be interpreted as indicative. However, we are confident that our model reliably captures the timescale of response, and therefore, despite uncertainties in the exact timing and magnitude, the predicted sediment patterns are expected under large-scale nourishment scenarios.

Within the work presented, our exclusive focus on two locations (Monster and Katwijk) was intentional to maintain conciseness in the results. The model used requires input parameters that are tuned for these locations. Other regions will react differently to nourishment, influenced by factors such as sediment type, the local wave climate and erosion rate. Although outcomes are expected to be qualitatively similar with a comparable methodology, the timing and extent of profile changes are likely to differ. In cases of similar nourishment design, the dispersion of nourished sand is generally faster when the sediment used is finer (Ludka et al., 2016), when the hydrodynamic climate is more energetic (Hamm et al., 2002) and when longshore erosion rates are larger. Moreover, if the nourished stretch of coast is bounded in either longshore or cross-shore directions, either naturally or by man-made structures, this may reduce the strength or limit of sand dispersion.

The strategies presented in this study serve as a framework for the current analysis, rather than a definitive set of options. Our scenarios assume the continuation of a chosen policy over half a century, revealing disproportionate outcomes such as the accumulation of large volumes of sand in the proactive scenarios. In real-world coastal management, any strategy leading to such undesirable changes would almost certainly be subject to revision along the way. Moreover, while our exploration is confined to the boundaries of laterally uniform nourishment strategies, there are numerous other options for coastal protection to consider. These alternatives may include different sandy approaches, such as pipeline or feeder nourishments, as well as ‘hard’ protection measures such as seawalls and dikes. The selection of a particular strategy in practice will include the morphological effects outlined in this work as well as socio-economic and ecologic aspects (Hanson et al., 2002). Taking a step further, the inquiry into how the coast shall be protected may extend to more fundamental considerations, such as determining

the threshold of sea level rise under which our coast can and should be maintained in its present form (Haasnoot et al., 2020) and when a retreat or managed realignment policy is to be favoured.

5. Conclusions

In the face of accelerated sea level rise, policymakers may consider different nourishment strategies involving larger sand volumes. High individual nourishment volumes or short return periods can lead to ineffective sand redistribution, whereby it may take decades for sand to reach slower-responding areas, typically farther from the nourishment site and at greater depths. The present study quantifies subsequent effects, including profile steepening, reduced nourishment lifetimes, and challenges in achieving strategic operational objectives, which are minimally addressed in current literature. Two common nourishment strategies were simulated with the cross-shore morphological model Crocodile over a 50-year timespan under different rates of sea level rise; the hold-the-line approach as reactive approach with minimal sand usage, and the sand balance approach as proactive option to elevate the coastal system, stretching seaward as deep as MSL-20 m, along with sea level rise.

An intercomparison between these strategies highlights the impact of strategy selection on sand volume usage. In the coming 50 years, the proactive strategy requires up to 6 times more sand than present-day volumes (*SLRr2*) to mitigate high sea level rise rates (*SLRr32*). The reactive hold-the-line strategy, in contrast, uses much less sand, requiring 30% less sand under low sea level rise rates (*SLRr2*) and 75% times less under high sea level rise rates (*SLRr32*). This underscores the importance of sand availability and economic considerations in strategy selection.

The simulations show that when high volumes of sand are applied, sand dispersion rates prove too slow for complete redistribution across the profile, leading to sand accumulation in the upper, nourished part of the profile over time. This effect increases with nourishment volume and duration of the nourishment strategy. In particular, the lower shoreface is hardly influenced by nourishments placed in the active profile. For example, a 50-year beach nourishment strategy under *SLRr8* leads to profile steepening by 23% in the proactive simulation and 16% in the reactive case. This profile steepening highlights a limitation in achieving the proactive strategy’s operational objective of elevating large areas, stretching seaward as deep as MSL-20 m, along with sea level rise. Under high rates of sea level rise, it may be necessary to reconsider operational objectives or nourishment design in such strategies, for instance by decreasing the profile depth to grow along with sea level rise.

The reactive hold-the-line simulations quantify how nourishment return periods reduce under accelerated sea level rise for coasts subject to varying erosion rates. Coastal areas with higher erosion rates see return periods drop to annual intervals, while less erosive coasts face the largest reduction in return periods and require up to four times more sand than at present under high sea level rise rates (*SLRr32*). The profile steepening leads to a supplementary reduction in return periods over the 50-year simulations by up to 30%. For the tested Dutch case this becomes significant after several decades of frequent nourishment and under sea level rise rates exceeding 8 mm/yr.

The projections of nourishment strategies discussed in this study provide insights into the relationships between man-made alterations to the sand budget and cross-shore dynamics. These relationships are instrumental in the formulation of future nourishment strategies and highlight the importance of optimizing these strategies to account for sea level rise.

CRediT authorship contribution statement

Tosca Kettler: Writing – original draft, Visualization, Validation, Software, Methodology, Investigation, Formal analysis, Data curation, Conceptualization. **Matthieu de Schipper:** Writing – review & editing,

Supervision, Project administration, Funding acquisition, Conceptualization. **Arjen Luijendijk**: Writing – review & editing, Supervision.

Declaration of competing interest

The authors declare the following financial interests/personal

Appendix

A1. Sea level rise scenarios

The sea level rise rates adopted in this research are based on expected sea level rise rates in the Netherlands over the next century, estimated by KNMI (2023) (Fig. A1). The KNMI (Royal Dutch Meteorological institute) adopted two IPCC scenarios to establish potential low-end and high-end scenario ranges of sea level rise. The low-emission scenario aligns with the second-lowest emission scenario of the IPCC (SSP1-2.6). This scenario would result in around 1.7 °C global warming in the latter half of this century compared to the late 19th century, consistent with the Paris Agreement. The high-emission scenario aligns with the high-emission scenario of the IPCC (SSP8.5), wherein emissions increase significantly until 2080 before stabilizing. The scenarios are not intended as predictions but span the probable range within which the long term mean water levels along the Dutch coast could change in the future. The actual climate change is likely to unfold somewhere between these two scenarios. The KNMI scenarios provide the context for the sea level rise rates adopted in this research. *SLRr2* scenario reflects conditions over the past decades, *SLRr4* serves as an estimate for the next decade, the *SLRr8* is anticipated several decades from now, and *SLRr16* may be approached near the end of this century under high emissions (Fig. 4). *SLRr32* is included to explore extremities.

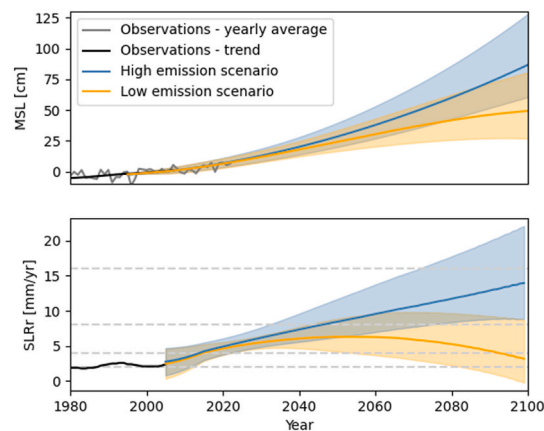


Fig. A1. – Scenarios for A) mean sea level (MSL) and B) rates of sea level rise (SLRr) for the Netherlands by KNMI (2023). The low emission scenario aligns with IPCC SSP1-2.6, the high emission scenario aligns with IPCC SSP8.5. Scenarios of rates of sea level rise applied in this study are indicated with grey dashed lines.

Data availability

Model code is available upon request from the author. The annual coastal data of the Dutch coast is available through <https://publicwiki.deltares.nl/display/OET/Dataset%20documentation%20JarKus>.

References

- Almar, R., Kestenare, E., Reyns, J., Jouanno, J., Anthony, E.J., Laibi, R., Hemer, M., Du Penhoat, Y., Ranasinghe, R., 2015. Response of the Bight of Benin (Gulf of Guinea, West Africa) coastline to anthropogenic and natural forcing, Part I: wave climate variability and impacts on the longshore sediment transport. *Continent. Shelf Res.* 110, 48–59. <https://doi.org/10.1016/j.csr.2015.09.020>.
- Beck, T.M., Rosati, J.D., Rosati, J., 2012. An Update on Nearshore Berms in the Corps of Engineers: Recent Projects and Future Needs.
- Bendixen, M., Best, J., Hackney, C., Iversen, L.L., 2019. Time is running out for sand. *Nature* 571 (7763), 29–31. <https://doi.org/10.1038/d41586-019-02042-4>.
- Brand, E., Ramaekers, G., Lodder, Q., 2022. Dutch experience with sand nourishments for dynamic coastline conservation – an operational overview. *Ocean Coast Manag.* 217 (December 2021), 106008. <https://doi.org/10.1016/j.ocecoaman.2021.106008>.
- Bruun, P., 1954. Coast erosion and the development of beach profiles. In: *Beach Erosion Board Technical Memorandum*, vol. 44. US Beach Erosion Board.
- Bruun, P., 1962. Sea-level rise as a cause of shore erosion. *J. Waterw. Harb. Div.* 88 (1), 117–132.
- Chen, W.L., Dodd, N., 2019. An idealised study for the evolution of a shoreface nourishment. *Continent. Shelf Res.* 178 (January), 15–26. <https://doi.org/10.1016/j.csr.2019.03.010>.
- Chen, W.L., Dodd, N., 2021. A nonlinear perturbation study of a shoreface nourishment on a multiply barred beach. *Continent. Shelf Res.* 214 (July 2020), 104317. <https://doi.org/10.1016/j.csr.2020.104317>.
- Coelho, C., Larson, M., Hanson, H., 2017. Simulating cross-shore evolution towards equilibrium of different beach nourishment schemes. *Coastal Dynamics* 1732–1746. June.
- Cooke, B.C., Jones, A.R., Goodwin, I.D., Bishop, M.J., 2012. Nourishment practices on Australian sandy beaches: a review. *J. Environ. Manag.* 113, 319–327. <https://doi.org/10.1016/j.jenvman.2012.09.025>.
- De Schipper, M.A., De Vries, S., Stive, M., De Zeeuw, R., Rutten, J., Ruessink, G., Aarninkhof, S., Van Gelder-Maas, C., 2014. Morphological development of a mega-nourishment; first observations at the sand engine. *Coastal Engineering Proceedings* 1 (34), 73. <https://doi.org/10.9753/icce.v34.sediment.73>.
- de Schipper, M., de Vries, S., Mil-Homens, J., Reniers, A., Ranasinghe, R., Stive, M., 2015. Initial volume losses at nourished beaches and the effect of surfzone slope. *The Proceedings of the Coastal Sediments 2015*. https://doi.org/10.1142/9789814689977_0050.
- De Vriend, H.J., Stive, M.J.F., Nicholls, R.J., Capobianco, M., 1993. Cross-shore spreading of shore nourishment. In: Bruun, P. (Ed.), *Proc. Hilton Head Island Coastal Symposium*, pp. 175–179.
- Dean, R.G., 1991. Equilibrium beach profiles: characteristics and applications. *J. Coast Res.* 1, 53–84. <https://www.jstor.org/stable/4297805>.
- Defeo, O., McLachlan, A., Schoeman, D.S., Schlacher, T.A., Dugan, J., Jones, A., Lastra, M., Scapini, F., 2009. Threats to sandy beach ecosystems: a review. *Estuar. Coast Shelf Sci.* 81 (1), 1–12. <https://doi.org/10.1016/j.ecss.2008.09.022>.
- Dillingh, D., Stolk, A., 1989. A Short Review of the Dutch Coast. *GWIO-89-004*.
- Duan, Z., Chen, J., Jiang, C., Liu, X., Zhao, B., 2020. Experimental study on uniform and mixed bed-load sediment transport under unsteady flow. *Appl. Sci.* 10 (6). <https://doi.org/10.3390/app10062002>.

- Faraci, C., Scandura, P., Foti, E., 2013. Bottom profile evolution of a perched nourished beach. *J. Waterw. Port. Coast. Ocean Eng.* 140 (5), 04014021. [https://doi.org/10.1061/\(ASCE\)WW.1943-5460.0000253](https://doi.org/10.1061/(ASCE)WW.1943-5460.0000253).
- Gijsman, R., Visscher, J., Schlurmann, T., 2018. A method to systematically classify design characteristics of sand nourishments. *Coastal Engineering Proceedings* 36, 95. <https://doi.org/10.9753/icce.v36.papers.95>.
- Haasnoot, M., Kwadijk, J., Van Alphen, J., Le Bars, D., Van Den Hurk, B., Diermanse, F., Van Der Spek, A., Oude Essink, G., Delsman, J., Mens, M., 2020. Adaptation to uncertain sea-level rise; how uncertainty in Antarctic mass-loss impacts the coastal adaptation strategy of The Netherlands. *Environ. Res. Lett.* 15 (3), 034007. <https://doi.org/10.1088/1748-9326/ab666c>.
- Hamm, L., Capobianco, M., Dette, H.H., Lechuga, A., Spanhoff, R., Stive, M.J.F., 2002. A summary of European experience with shore nourishment. *Coastal Engineering* 47 (2), 237–264. [https://doi.org/10.1016/S0378-3839\(02\)00127-8](https://doi.org/10.1016/S0378-3839(02)00127-8).
- Hands, E.B., Allison, M.C., 1991. Mound migration in deeper water and methods of categorizing active and stable berm depths. In: *Proceedings of a Specialty Conference on Quantitative Approaches to Coastal Sediment Processes*, vol. 2.
- Hanson, H., Brampton, A., Capobianco, M., Dette, H.H., Hamm, L., Lastrup, C., Lechuga, A., Spanhoff, R., 2002. Beach nourishment projects, practices, and objectives—a European overview. *Coastal Engineering* 47 (2), 81–111. [https://doi.org/10.1016/S0378-3839\(02\)00122-9](https://doi.org/10.1016/S0378-3839(02)00122-9).
- Hinton, C., Nicholls, R.J., 1998. Spatial and temporal behaviour of depth of closure along the Holland coast. *Proc. Coast. Eng. Conf.* 3, 2913–2925. <https://doi.org/10.1061/9780784404119.221>.
- Kettler, T., de Schipper, M., Luijendijk, A., 2024. Simulating decadal cross-shore dynamics at nourished coasts with Crocodile. *Coastal Engineering* 190, 104491. <https://doi.org/10.1016/J.COASTALENG.2024.104491>.
- KNMI, 2023. *KNMI 23-klimaatscenario's Voor Nederland*.
- Liu, X., Luo, X., Lu, C., Zhang, G., Ding, W., 2024. The impact of foreshore slope on cross-shore sediment transport and sandbar formation in beach berm nourishment. *Water* 16 (15), 2212. <https://doi.org/10.3390/w16152212>.
- Lodder, Q.J., Slinger, J.H., Wang, Z.B., van Gelder, C., 2020. Decision making in Dutch coastal research based on coastal management policy assumptions. *Coast. Manag.* 2019, 291–300. <https://doi.org/10.1680/cm.65147.291>.
- Lodder, Q., Slinger, J., 2022. The 'Research for Policy' cycle in Dutch coastal flood risk management: the Coastal Genesis 2 research programme. *Ocean Coast Manag.* 219 (July 2021), 106066. <https://doi.org/10.1016/j.ocecoaman.2022.106066>.
- Ludka, B.C., Gallien, T.W., Crosby, S.C., Guza, R.T., 2016. Mid-El Niño erosion at nourished and unnourished Southern California beaches. *Geophys. Res. Lett.* 43 (9), 4510–4516. <https://doi.org/10.1002/2016GL068612>.
- Marinho, B., Coelho, C., Larson, M., Hanson, H., 2017. Simulating cross-shore evolution towards equilibrium of different beach nourishment schemes. *Coastal Dynamics* 1732–1746. <https://www.researchgate.net/publication/323583035>.
- McCarroll, R.J., Masselink, G., Valiente, N.G., Scott, T., Wiggins, M., Kirby, J.-A., Davidson, M., 2021. A rules-based shoreface translation and sediment budgeting tool for estimating coastal change: ShoreTrans. *Mar. Geol.* 435, 106466. <https://doi.org/10.1016/j.margeo.2021.106466>.
- Mulder, J.P.M., 2000. *Zandverliezen in Het Nederlandse Kuststelsysteem*.
- Nederbragt, G.J., 2006. *Zandvoorraden van het kuststelsysteem: onderbouwing van een conceptueel model met behulp van trends van de winst- en verliesposten over de periode 1973-1997*.
- Pang, W., Dai, Z., Ma, B., Wang, J., Huang, H., Li, S., 2020. Linkage between turbulent kinetic energy, waves and suspended sediment concentrations in the nearshore zone. *Mar. Geol.* 425, 106190. <https://doi.org/10.1016/j.margeo.2020.106190>.
- Pang, W., Ge, Z., Dai, Z., Li, S., Huang, H., 2021. The behaviour of beach elevation contours in response to different wave energy environments. *Earth Surf. Process. Landforms* 46 (2), 443–454. <https://doi.org/10.1002/esp.5036>.
- Rijkswaterstaat, 2020. *Kustgenese 2.0: Kennis Voor Een Veilige Kust*.
- Schipper, M. A. De, Ludka, B.C., Raubenheimer, B., Luijendijk, A.P., Schlacher, T.A., 2021. Beach nourishment has complex implications for the future of sandy shores. *Nat. Rev. Earth Environ.* 1–15. <https://doi.org/10.1038/s43017-020-00109-9>.
- Stive, M.J.F., de Vriend, H.J., 1995. Modelling shoreface profile evolution. *Mar. Geol.* 126 (1–4), 235–248. [https://doi.org/10.1016/0025-3227\(95\)00080-1](https://doi.org/10.1016/0025-3227(95)00080-1).
- Stive, M.J.F., Nicholls, R.J., de Vriend, H.J., 1991. Sea-level rise and shore nourishment: a discussion. *Coastal Engineering* 16 (1), 147–163. [https://doi.org/10.1016/0378-3839\(91\)90057-N](https://doi.org/10.1016/0378-3839(91)90057-N).
- Taal, M., Quataert, E., van der Spek, A., Huisman, B., Elias, E., Wang, Z., Vermeer, N., 2023. *Sedimentbehoefte Nederlands Kuststelsysteem Bij Toegenomen Zeespiegelstijging*.
- Torres, A., Brandt, J., Lear, K., Liu, J., 2017. A looming tragedy of the sand commons. *Science* 357 (6355), 970–971. <https://doi.org/10.1126/SCIENCE.AAO0503>.
- Valloni, R., Médit, M.B., 2007. Artificial beach nourishment projects in Italy. In: *Intervento Presentato Al Convegno 38th CONGRÉS CIESM Tenutosi a ISTANBUL Nel 9-13 Mars 2007*, p. 706, 706. https://ciesm.org/online/archives/abstracts/pdf/38/CIESM_Congress_2007_Istanbul_article_0706.pdf.
- van der Spek, A., Lodder, Q.J., 2015. A new sediment budget for The Netherlands; the effects of 15 years of nourishing (1991-2005). *The Proceedings of the Coastal Sediments 2015*. https://doi.org/10.1142/9789814689977_0074.
- Van Koningsveld, M., Mulder, J.P.M., 2004. Sustainable coastal policy developments in The Netherlands. A systematic approach revealed. *J. Coast Res.* 20 (2), 375–385. [https://doi.org/10.2112/1551-5036\(2004\)020\[0375:SCPDIT\]2.0.CO;2](https://doi.org/10.2112/1551-5036(2004)020[0375:SCPDIT]2.0.CO;2).
- Wijnberg, K.M., Terwindt, J.H.J., 1995. Extracting decadal morphological behaviour from high-resolution, long-term bathymetric surveys along the Holland coast using eigenfunction analysis. *Mar. Geol.* 126 (1–4), 301–330. [https://doi.org/10.1016/0025-3227\(95\)00084-C](https://doi.org/10.1016/0025-3227(95)00084-C).
- Yao, Z., Chen, J., Jiang, C., Liang, H., Wu, Z., Deng, B., Long, Y., Bian, C., 2024. Experimental analysis of the changes in coral sand beach profiles under regular wave conditions. *J. Mar. Sci. Eng.* 12 (2). <https://doi.org/10.3390/jmse12020287>.